Structure and Kinematics of the central BLR in AGN

Wolfram Kollatschny, Göttingen

Andrevlje, Serbia, 2012

University Observatory

Institute for Astrophysics

Scale Sizes of an AGN

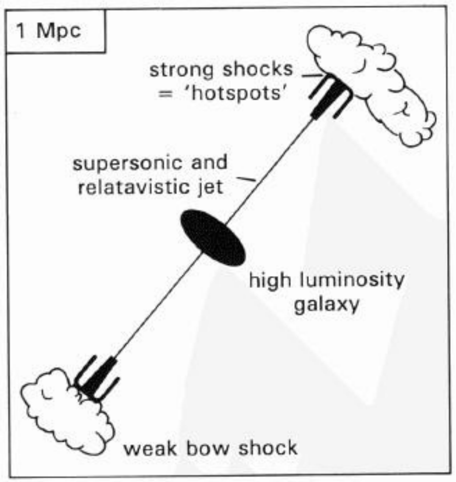

Extended radio sources — shown is an FRII source with an edge-brightened structure. The FRIs have lower jet velocities and fade-out to the ends.

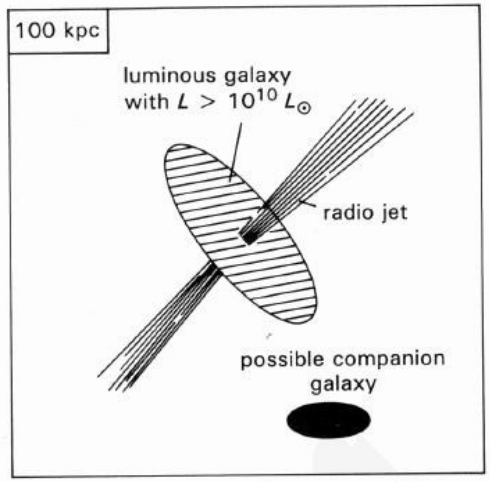

The host galaxy. Although shown as an early type galaxy with a smooth profile, it could also be highly irregular with multiple nuclei as a result of merging.

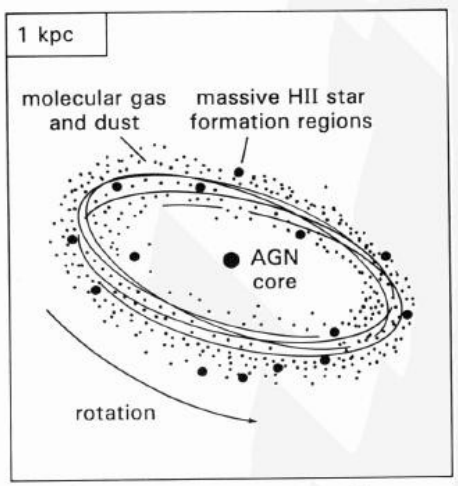

The central kpc star formation disk. This strong far infrared emitting zone might be fed by a bar structure, as seems to be the case for NGC1068.

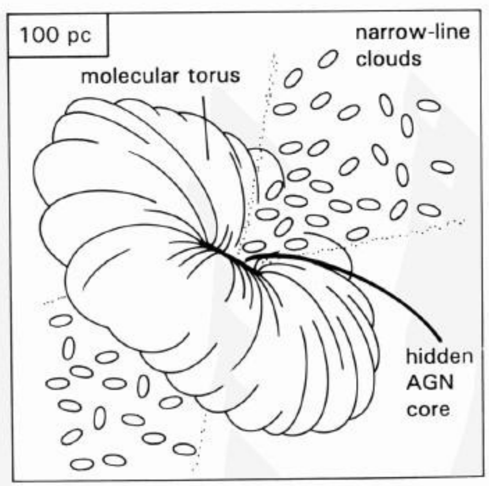

The narrow-line region comprising small but numerous clouds of the interstellar medium ionized by the central AGN core.

Fig. 9.9 Cartoon of the representative scale sizes of an AGN. How we eventually see the object depends on a number of parameters, the main one being the orientation of the obscuring torus with respect to the observer. (Adapted from Blandford, *Active Galactic Nuclei*, Saas-Fee Advanced Course 20, Springer–Verlag, 1990.)

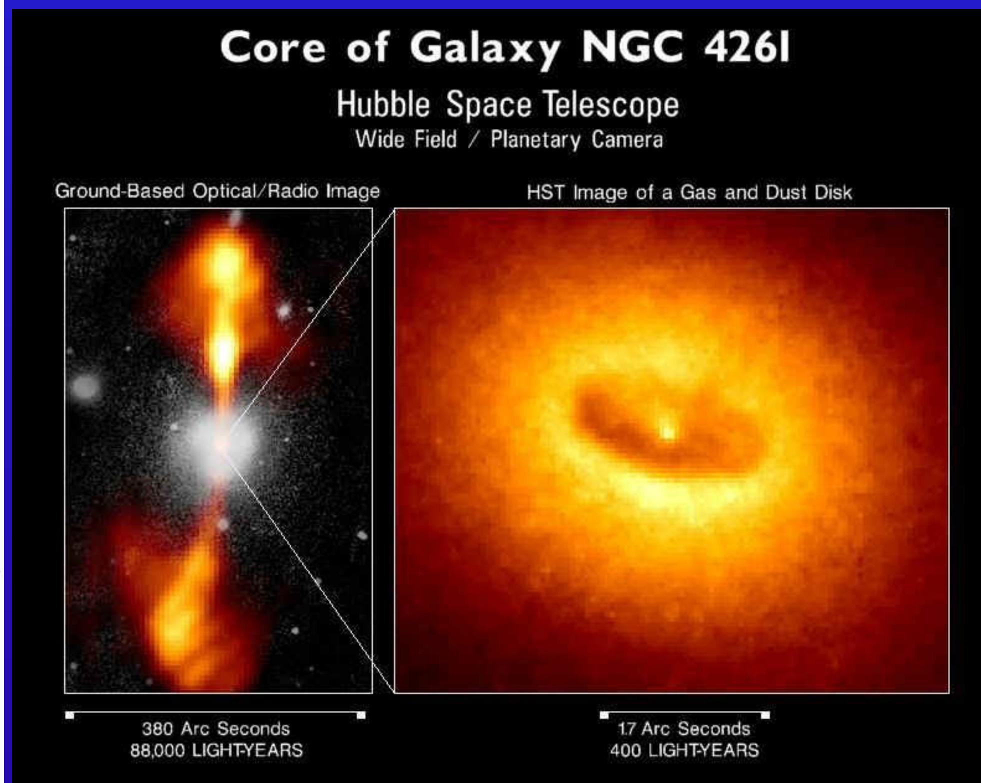

R. Blandford

Broad Line Region Size?

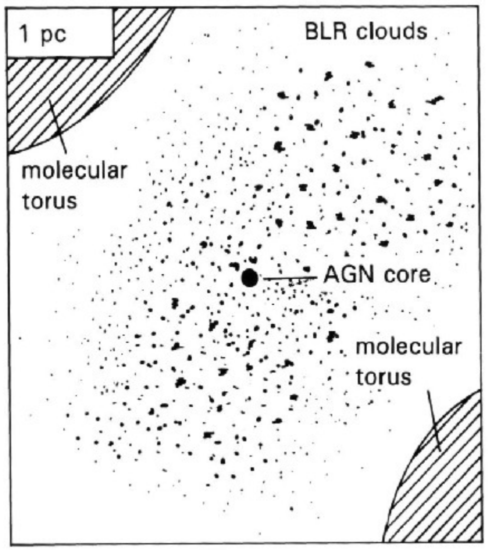

The outer extent of the broad-line region and the deep-walled molecular torus which can provide an effective shield of the central AGN, depending on the relative orientation of the observer.

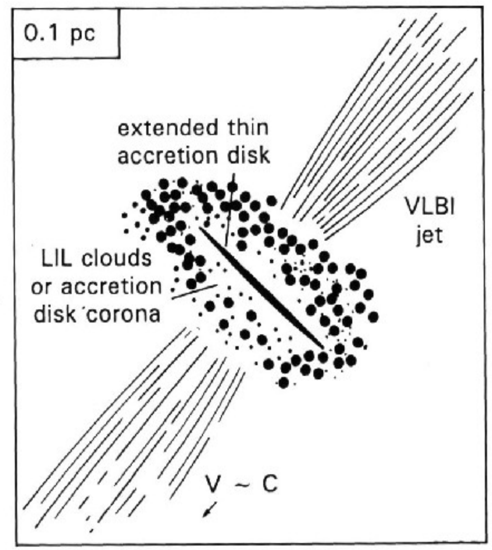

Inside the molecular torus — the VLBI jet becomes self-absorbed closer in, and the low ionization lines of the BLR, which might be the corona of the accretion disk.

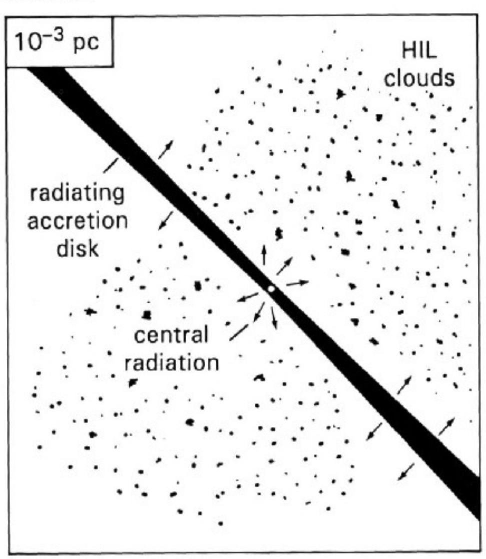

The accretion disk which radiates strongly at UV and optical wavelengths. The high ionization clouds of the BLR are excited by the central continuum radiation field.

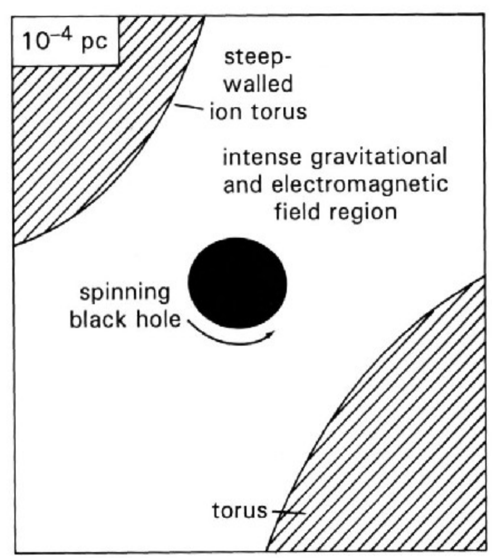

The black hole. The Schwarzschild radius for a $10^8\ M_\odot$ black hole is 2 AU (10^{-5} pc). The spin will introduce twisted magnetic field lines and particle acceleration.

radius:
- 10^{-4} ...10^{-1} pc
- 1 .... 100 light days

at a dist. of 50 Mpc (Virgo):
spatial resolution

4×10^{-5} ... 4×10^{-3} ''
(0.04 ... 4. mas)

unresolved

R. Blandford

Broad Line Region Structure, Kinematics?

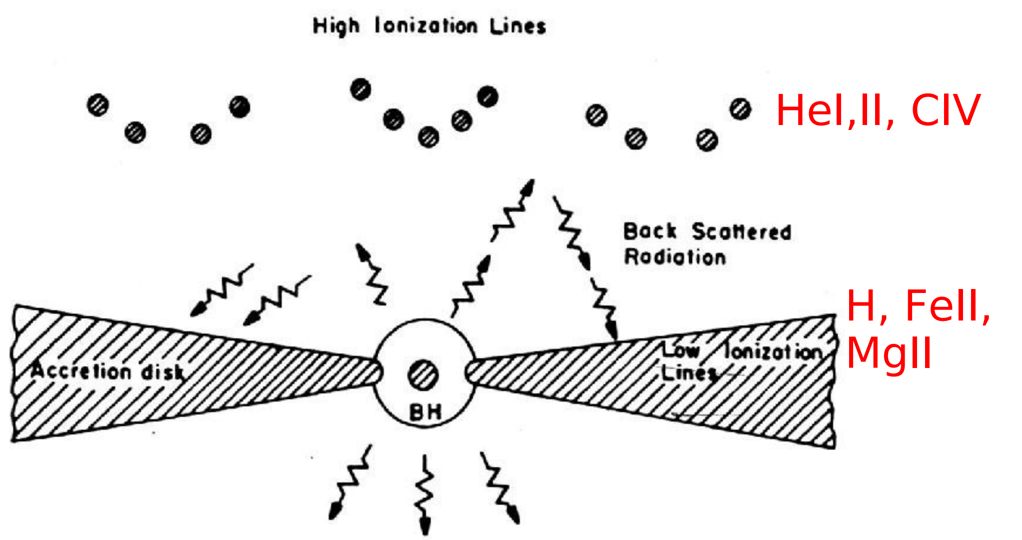

Fig. 13. A schematic two-component model for the BLR. The high ionization lines are emitted in a spherical system of clouds, and are excited by the direct ultraviolet radiation of the central source. The low ionization lines come mainly from the outer regions of the central disk, where most of the line excitation is due to back-scattered, hard ionizing photons. (After Collin-Souffrin, Perry and Dyson(1987), Collin-Souffrin (1987) and Dumont and Collin-Souffrin (1990))

464 EMMERING, BLANDFORD, & SHLOSMAN Vol. 385

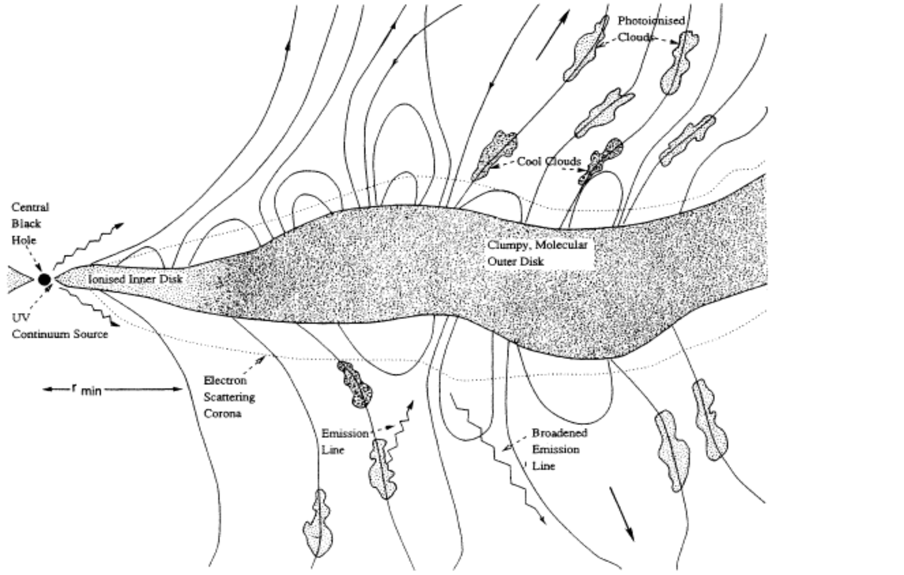

FIG. 1.—Schematic representation of magnetic accretion disk model for broad emission-line region. The accretion disk is ionized in the inner parts but neutral and probably molecular at large radius. Small dense clouds of molecular gas can be radiatively accelerated away from the surface of the disk and flung centrifugally outward along the magnetic field to attain speeds several times the initial Keplerian velocities. When these clouds are exposed to the full UV photoionizing flux, they are heated to temperatures $T \sim 10^4$ K and produce the emission lines. It is possible that these line photons are subsequently scattered by $\sim 10^6$ K electrons, either within a corona or at the disk.

Two component BLR?

Collin-Souffrin et al., 1990

Radiatively accelerated clouds in hydromagnetic wind?

Emmering, Blandford, Shlosman,1992

AGN working model

NGC 3783

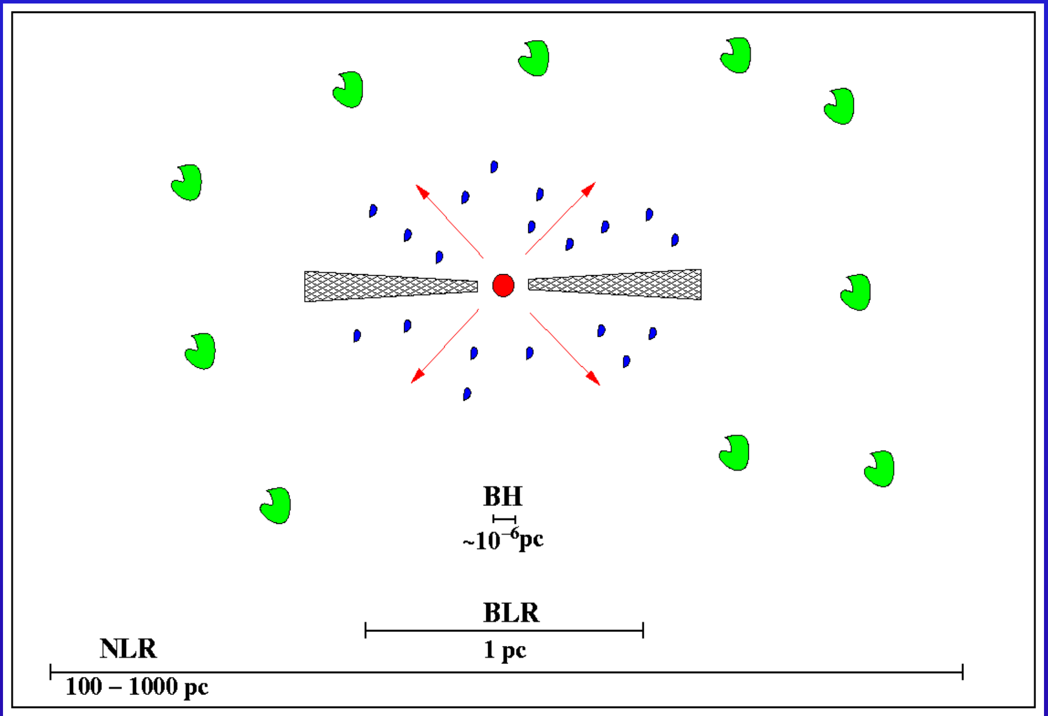

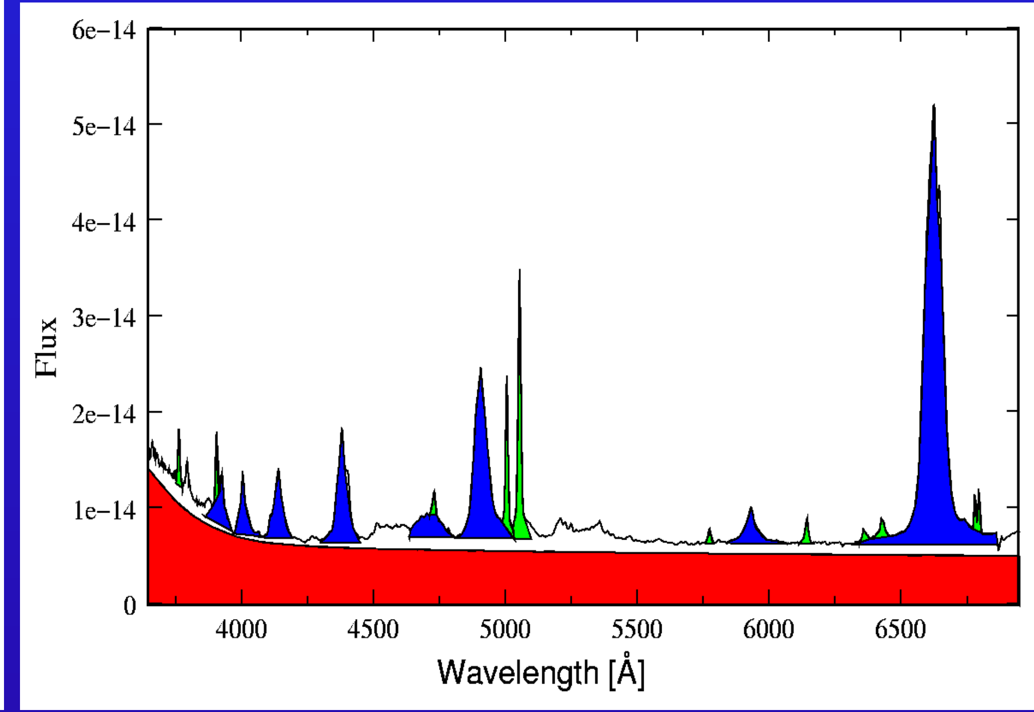

Central SMBH~10^8 M_O ~ 10^{13}cm: surrounded? by ionizing non-thermal source

Broad Line Region (<1pc): emission lines due to photo-ionization

Narrow Line Region (~100-1000pc): emission lines due to photo-ionization

geometry, kinematics?

Study of Variability, Study of Line Profiles

1) Study of integrated line and continuum variability:

- extension, structure of central BLR in AGN

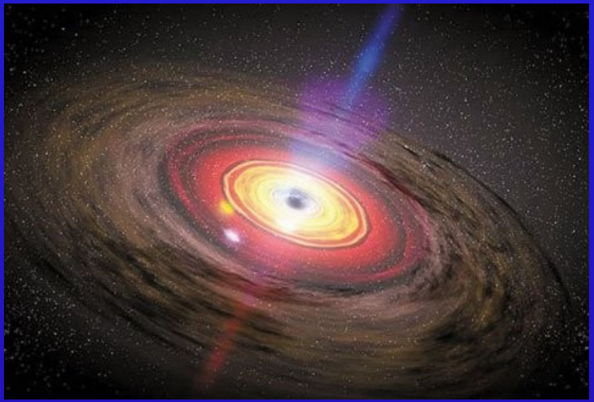

artist view

2) Study of line profile variability

- Geometry and Kinematics in the BLR

3) Study of general trends in line profiles

- Geometry and Kinematics in the BLR

- *central Black Hole Masses*

in NGC5548, Mrk110, 3C120, 3C390.3, AGN sample

Study of Variability, Study of Line Profiles

1) Study of integrated line and continuum variability:

- extension, structure of central BLR in AGN

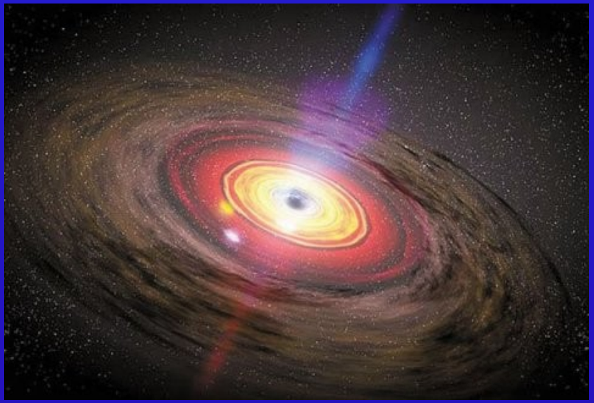

artist view

- *central Black Hole Masses*

in NGC5548, Mrk110, 3C120

High and low state spectra of NGC5548

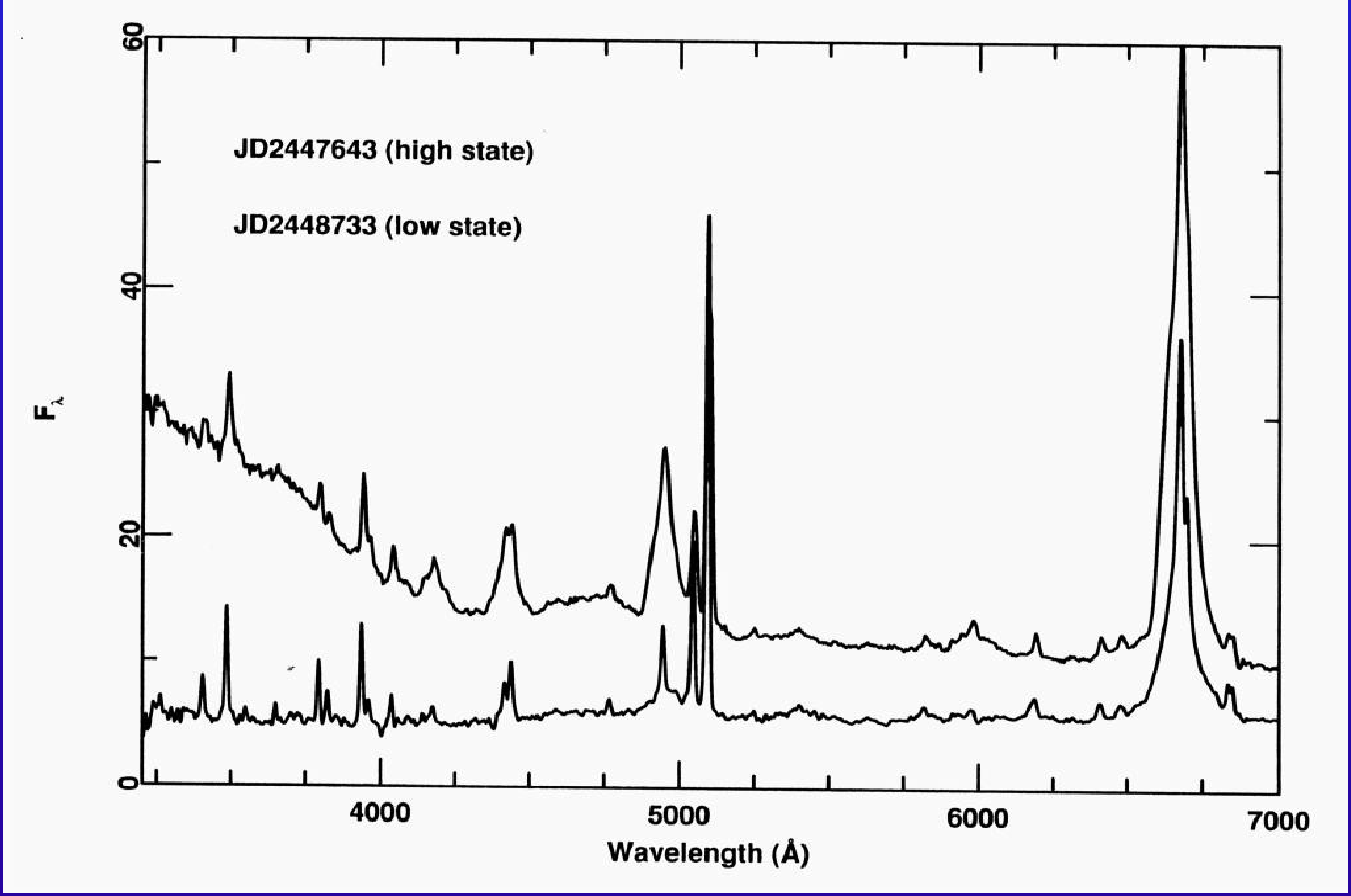

1989

1993

BLR: Idealized Model

Response of BLR clouds on continuum flashes

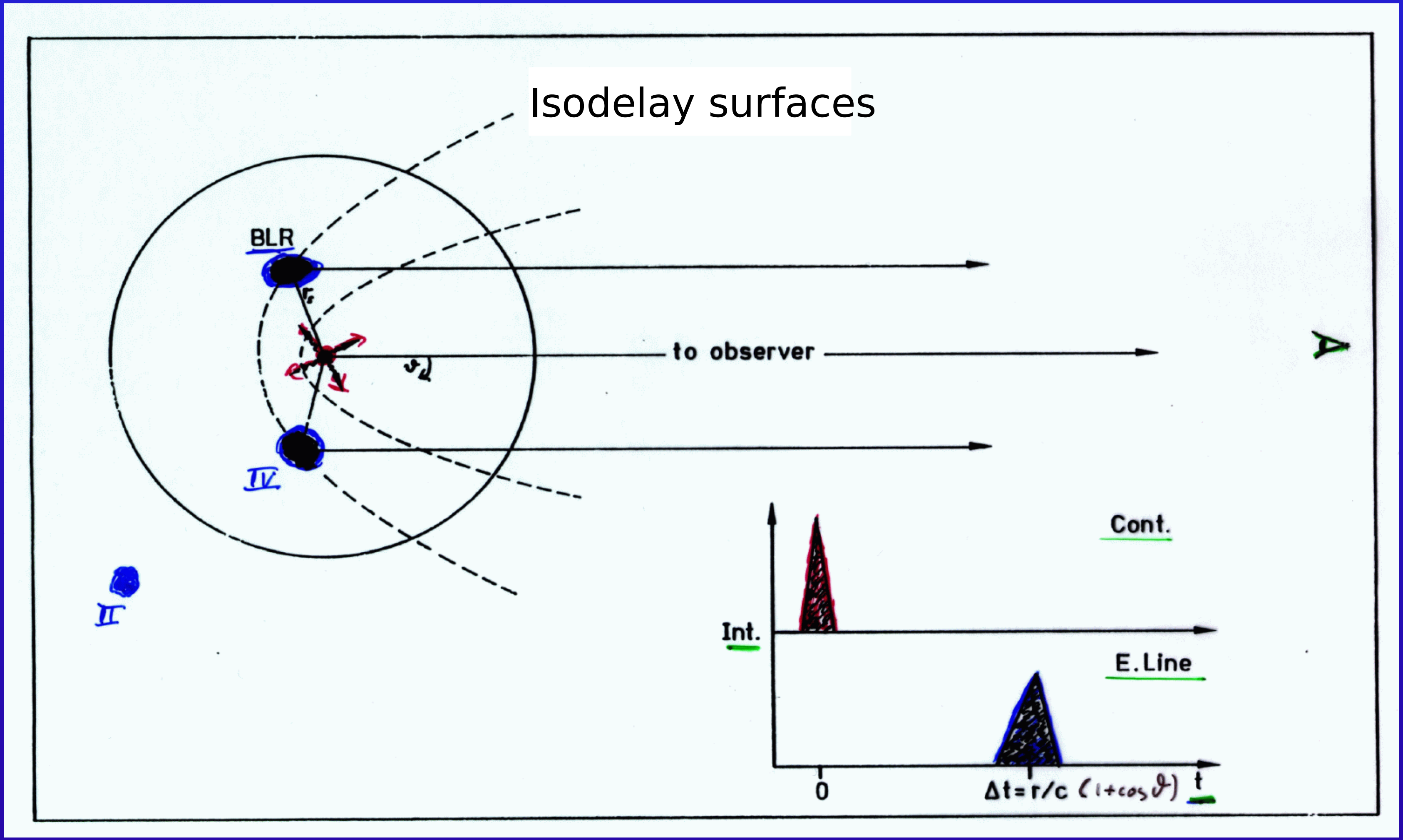

BLR stratification

Delay by light travel time effects

BLR: Continuum & integ. Hβ line variability

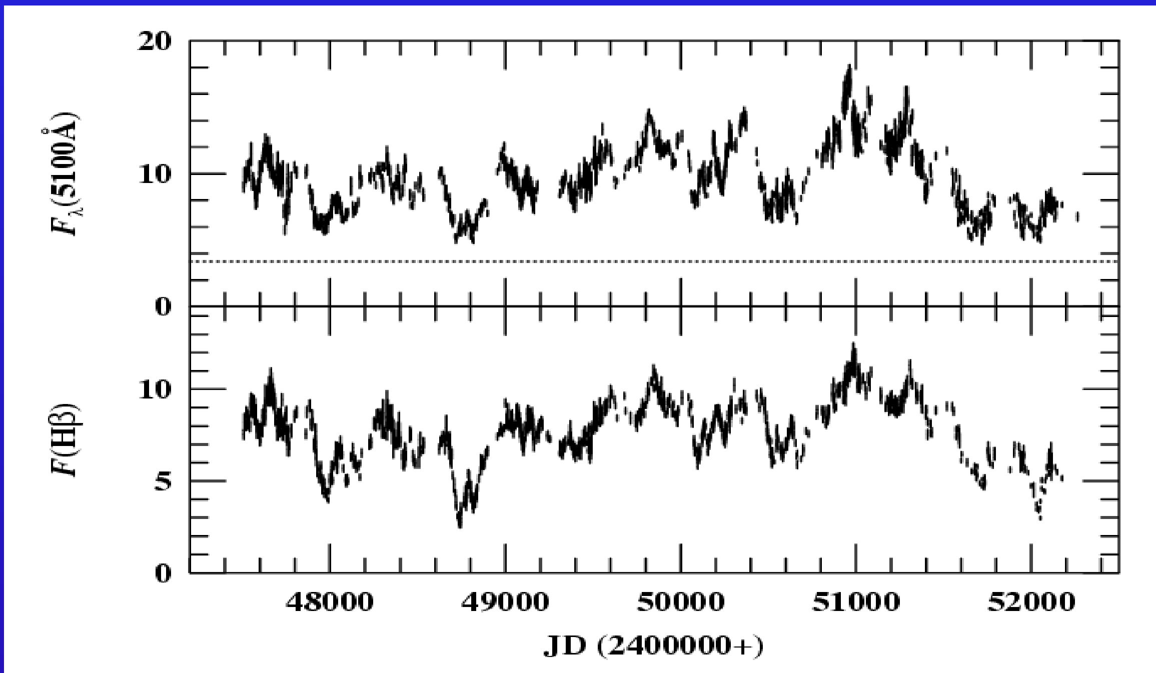

1989 - 2001

NGC 5548

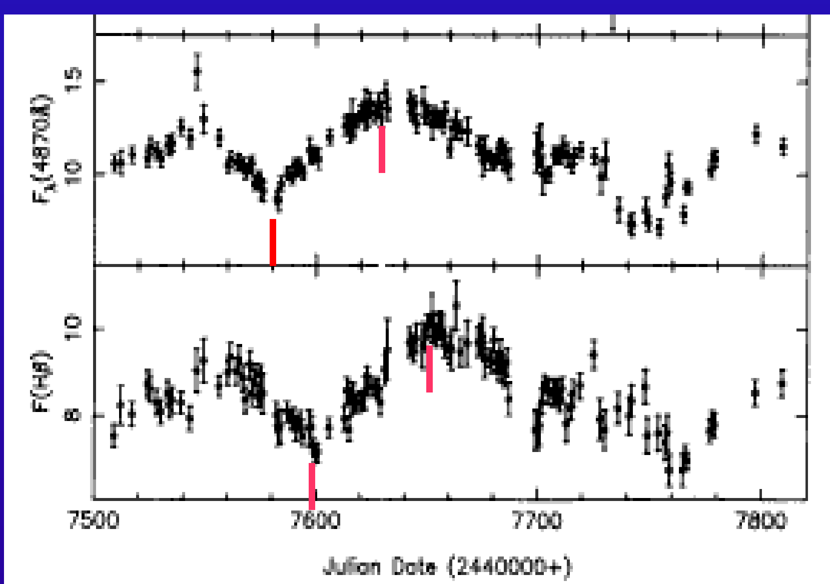

B. Peterson et al., 2002

Hβ delay ~ 20 light days

1989

BLR size and stratification in NGC5548

peak to peak
var. ampl.

lightcurves (1989)

ACF, CCF

opt. Cont.

0.56

Hβ

0.29

Hα

0.17

HeII

0.61

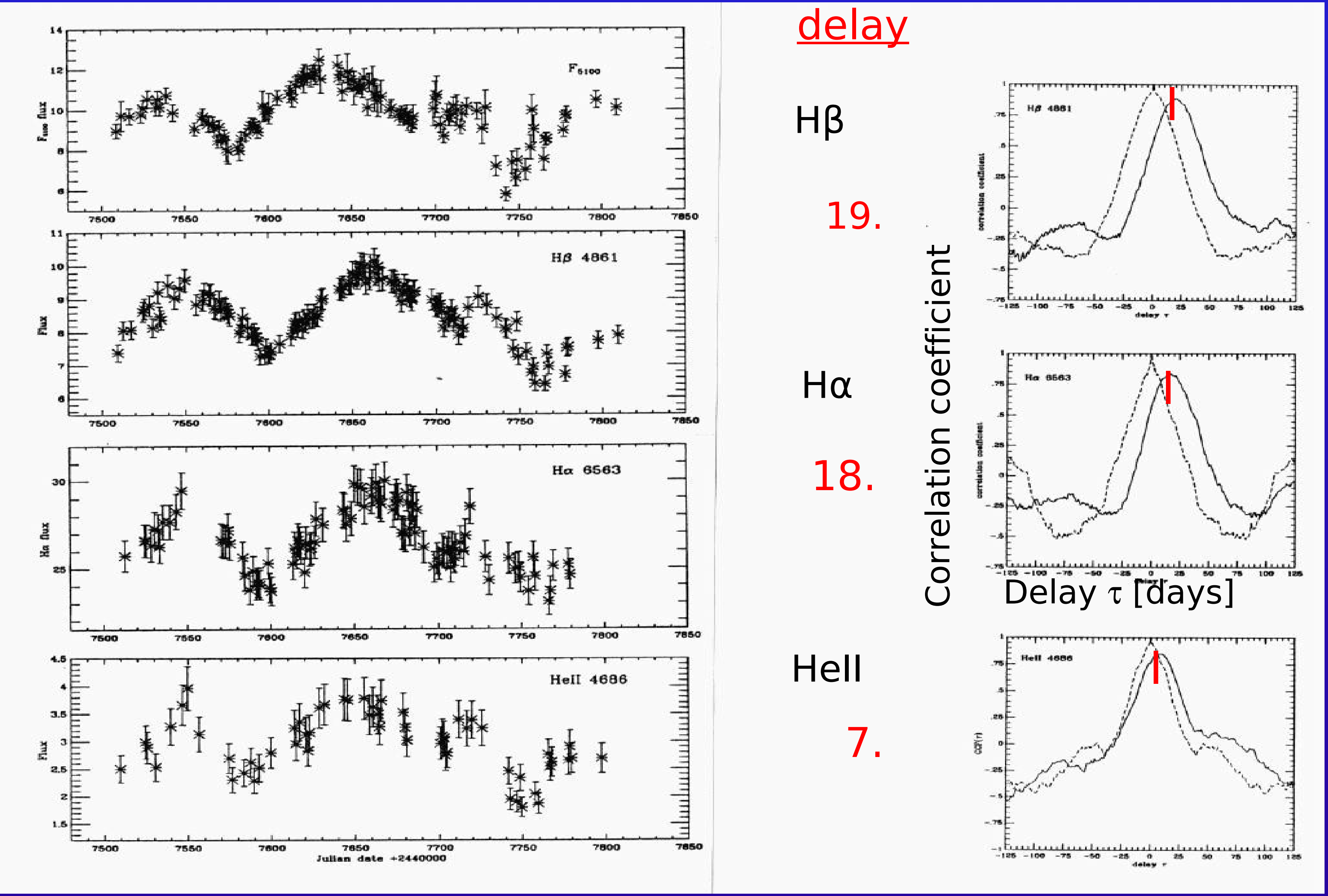

Dietrich, Kollatschny et al., 1994

BLR size and stratification in NGC5548

higher ionized lines: - broader line widths
- faster response

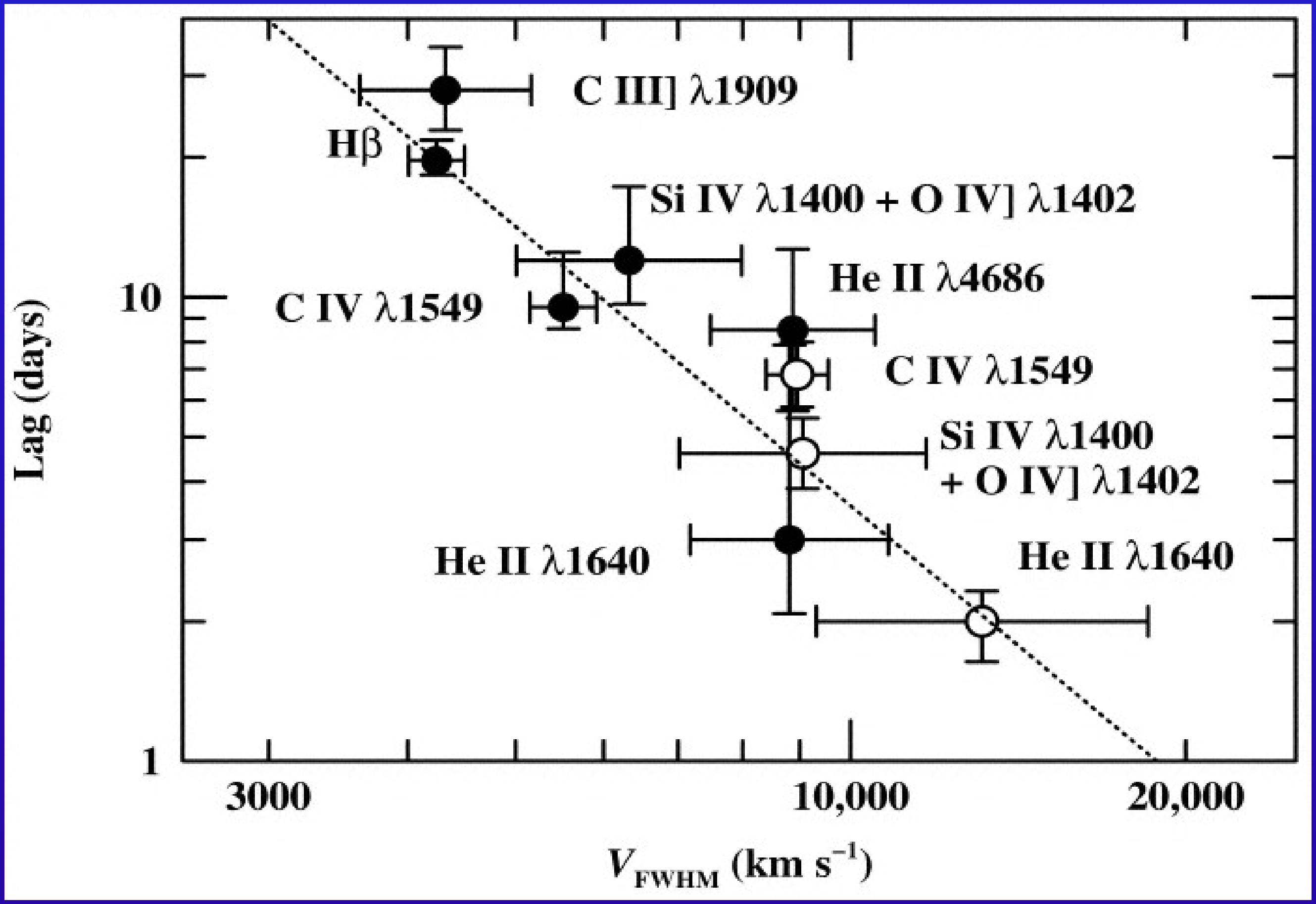

Time lag (CCFs centroids) for various emission lines

Peterson, Wandel, 1999

HET variability campaign of Mrk110

long-term continuum light curve

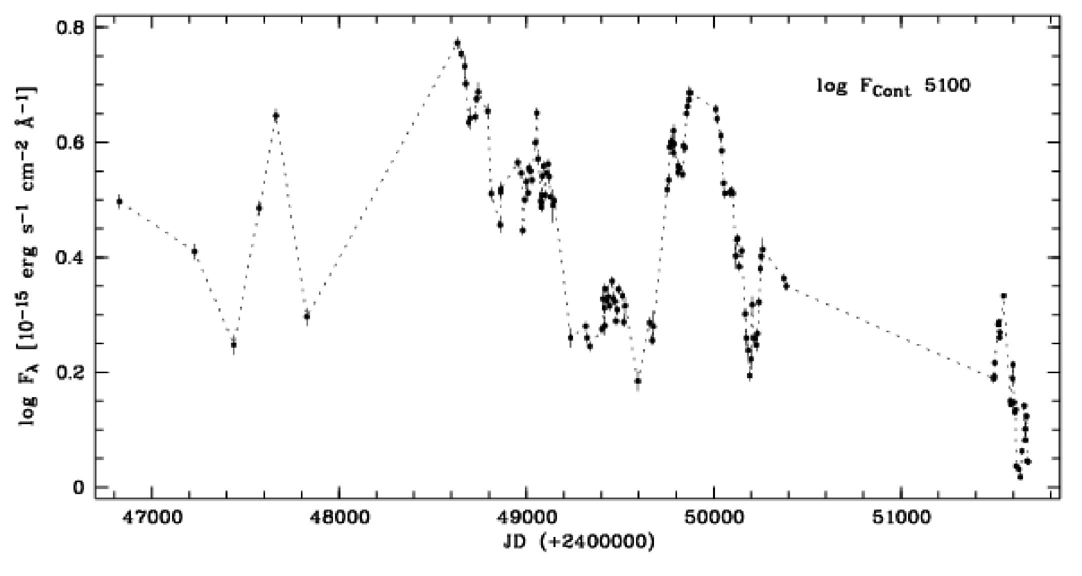

1987

2000

Mrk110 spectra taken between 1999 Nov. and 2000 May

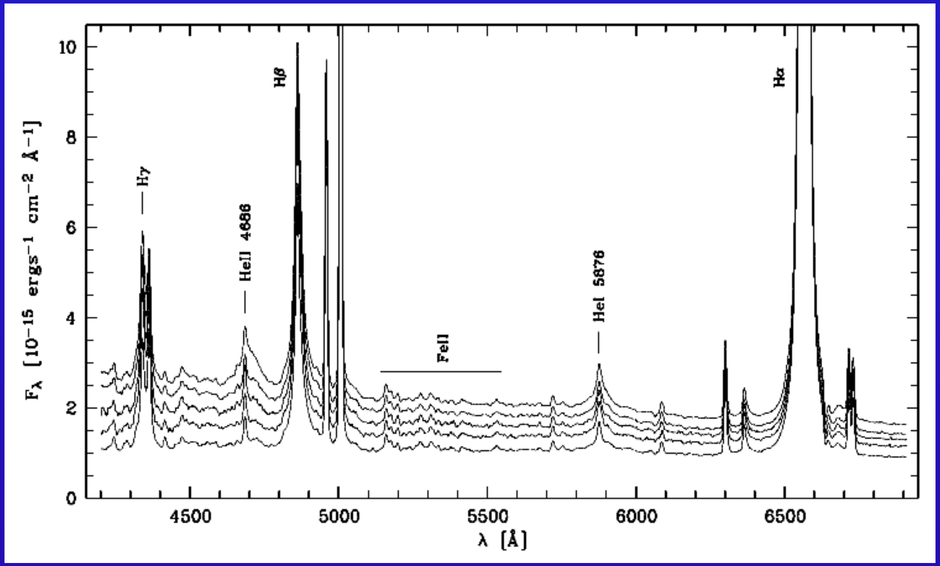

9.2m Hobby-Eberly Telescope
at McDonald Observatory
S/N >100

Hobby-Eberly Telescope (HET),McDonald

segmented 10m mirror

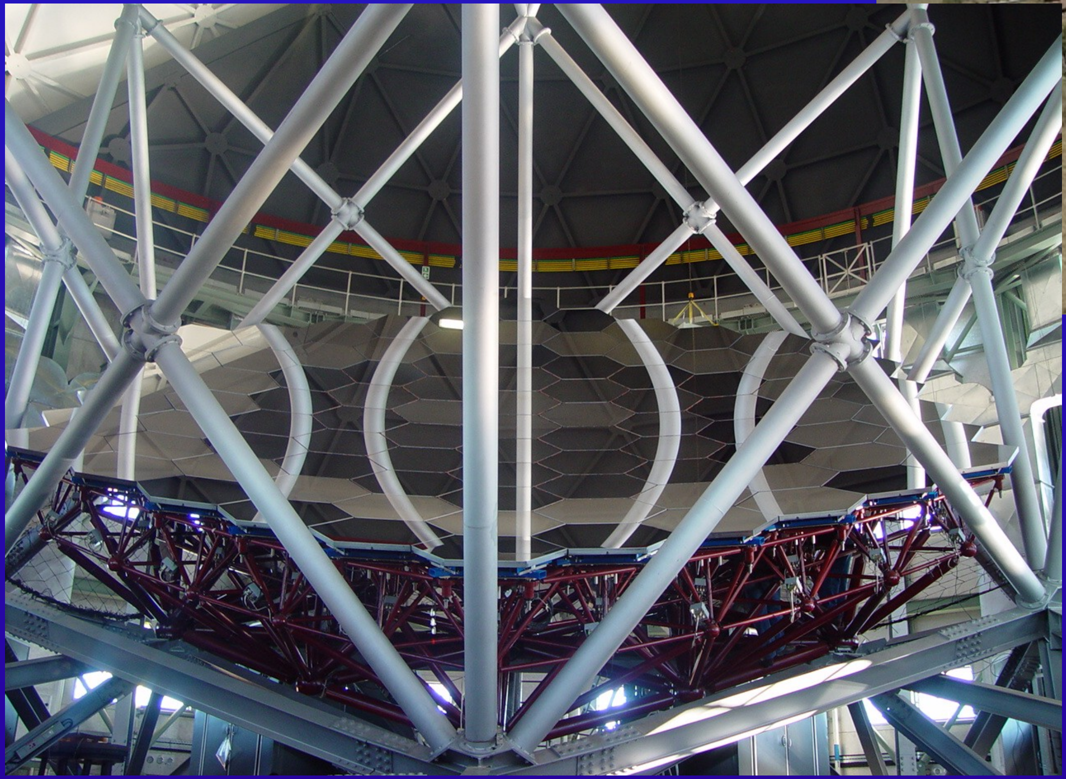

-Univ. of Texas at Austin
-Pennsylvania State Univ.
-Stanford Univ.
-Göttingen Univ.
-München Univ.

HET variability campaign of Mrk110

9.2m Hobby-Eberly Telescope at McDonald Observatory
S/N >100

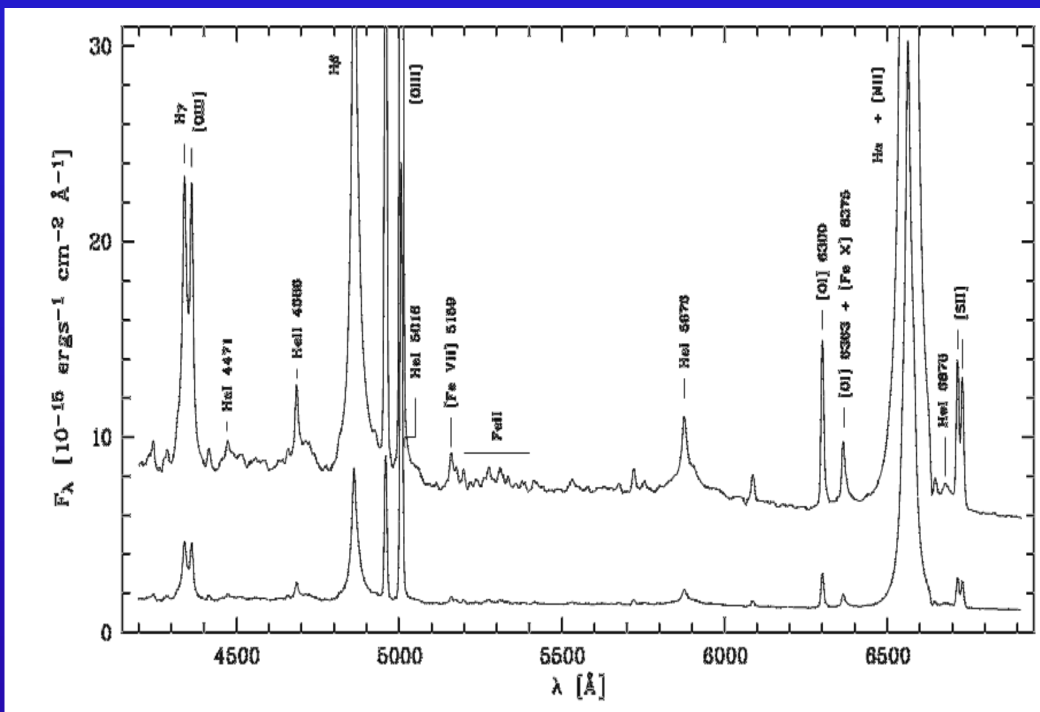

Mean spectrum of Mrk110
for 24 epochs from Nov. 1999 through
May 2000

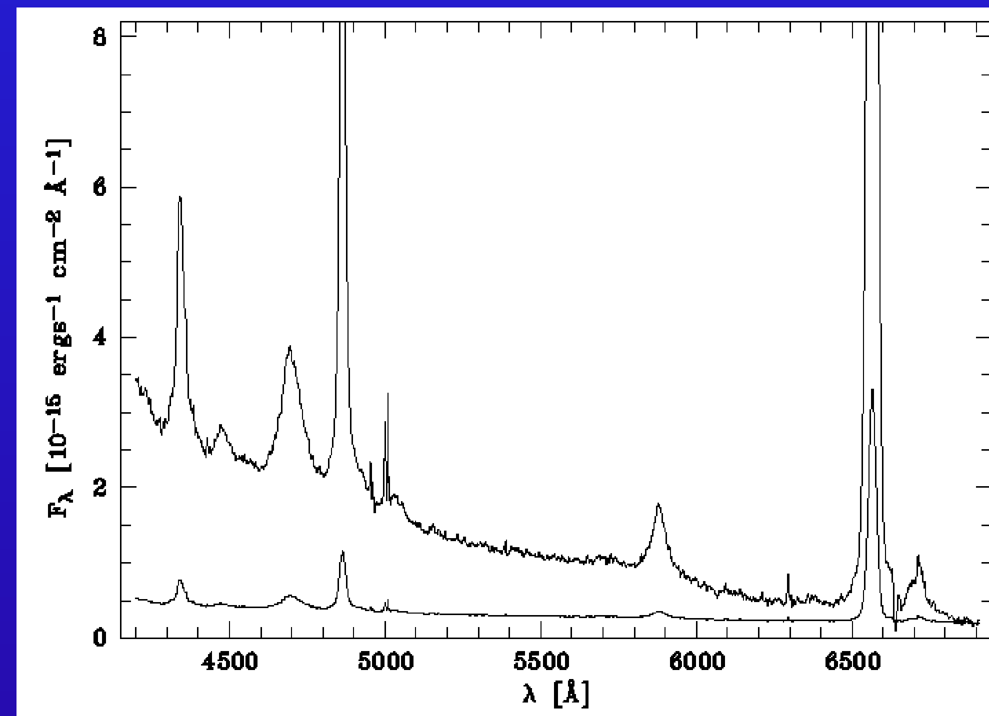

Rms spectrum

- the rms spectrum shows the variable part of the spectrum

Kollatschny et al., 2001

HET variability campaign of Mrk110

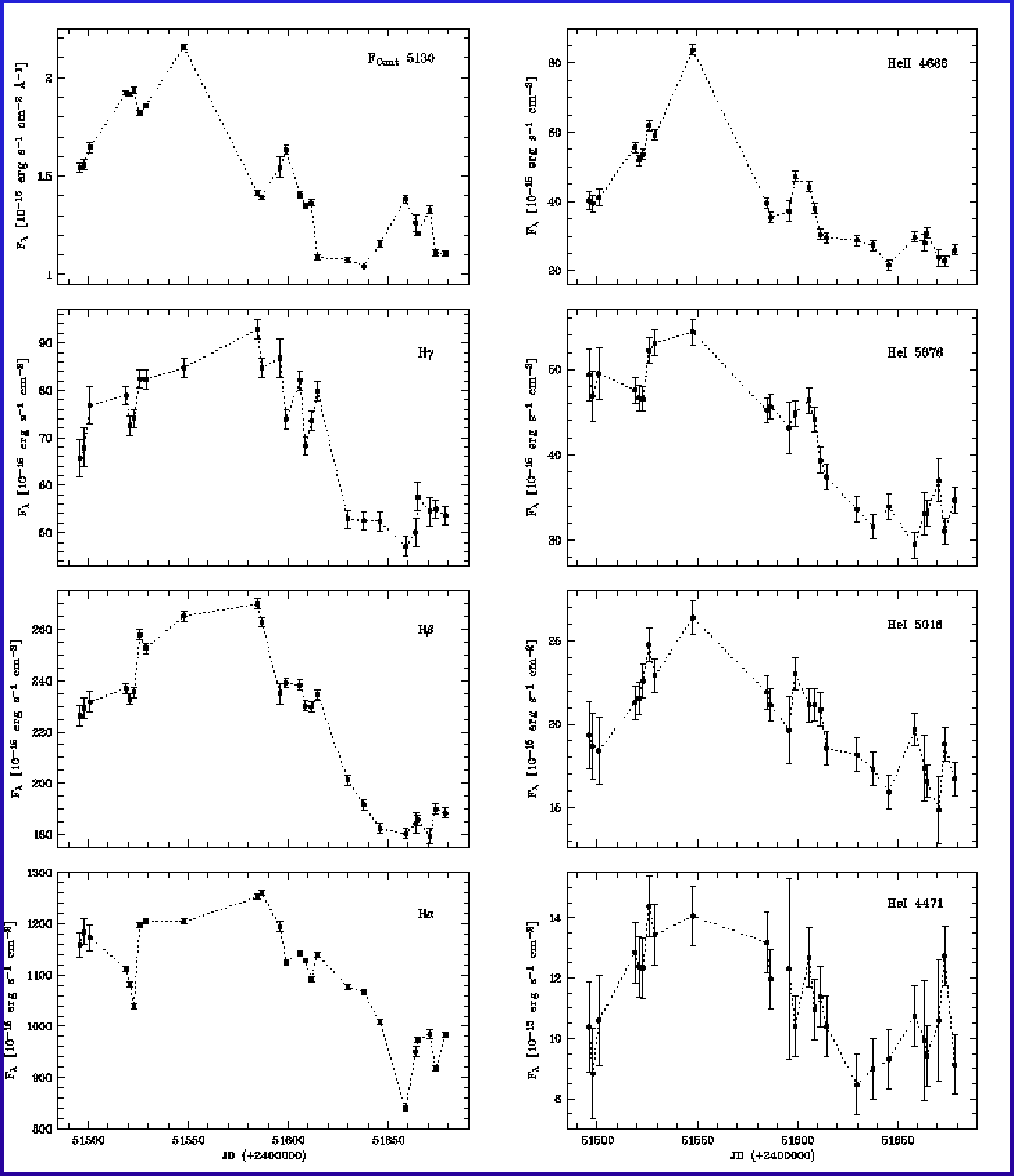

Continuum and integrated emission line (Balmer, HeII and HeI) light curves

1999 Nov. - 2000 May

Kollatschny et al., 2001

BLR size and structure - HET variab. campaign

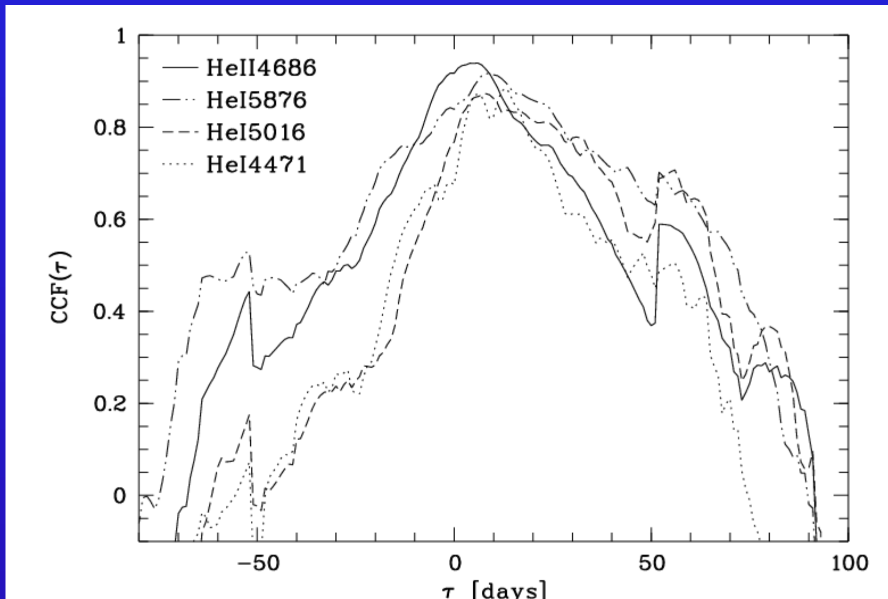

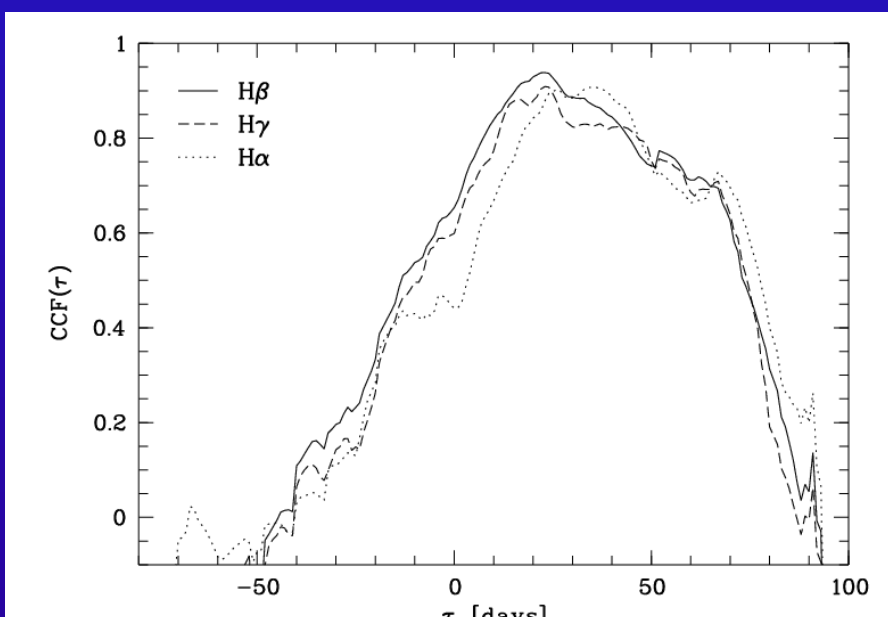

Mkn110

CCF functions of HeII, HeI and Balmer line light curves with continuum light curve.

Line (1)	τ_{cent} [days] (2)
HeIIλ4686	$3.9^{+2.8}_{-0.7}$
HeIλ4471	$11.1^{+6.0}_{-6.0}$
HeIλ5016	$14.3^{+7.0}_{-7.0}$
HeIλ5876	$10.7^{+8.0}_{-6.0}$
Hγ	$26.5^{+4.5}_{-4.7}$
Hβ	$24.2^{+3.7}_{-3.3}$
Hα	$32.3^{+4.3}_{-4.9}$

stratification

BLR size and stratification in Mrk110

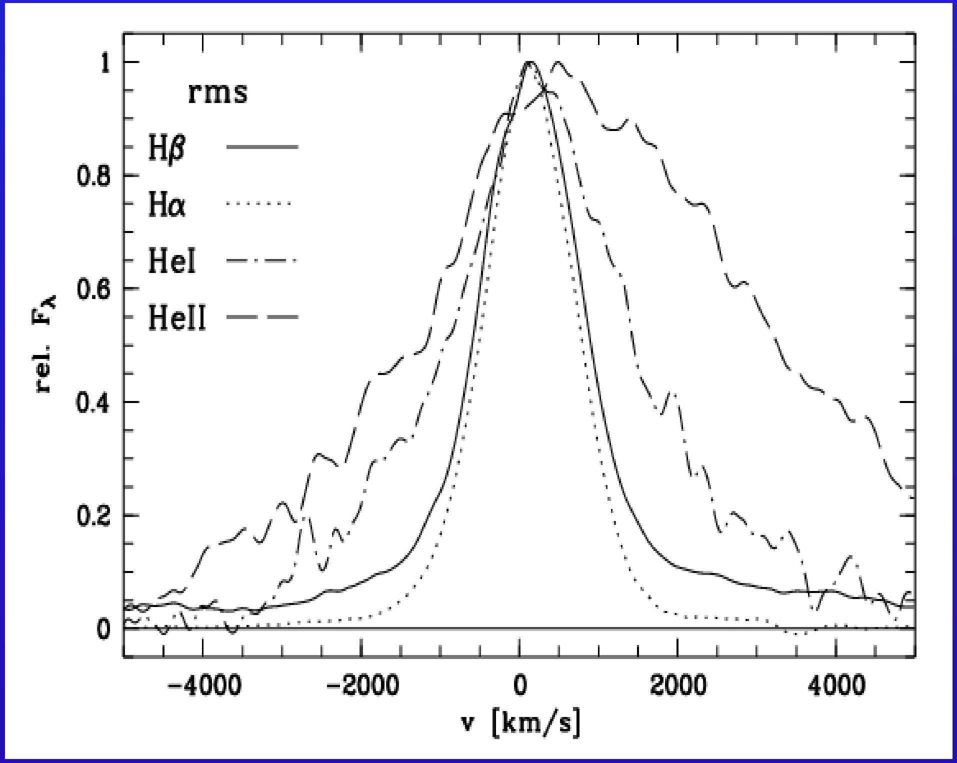

Normalized rms line profiles in velocity space

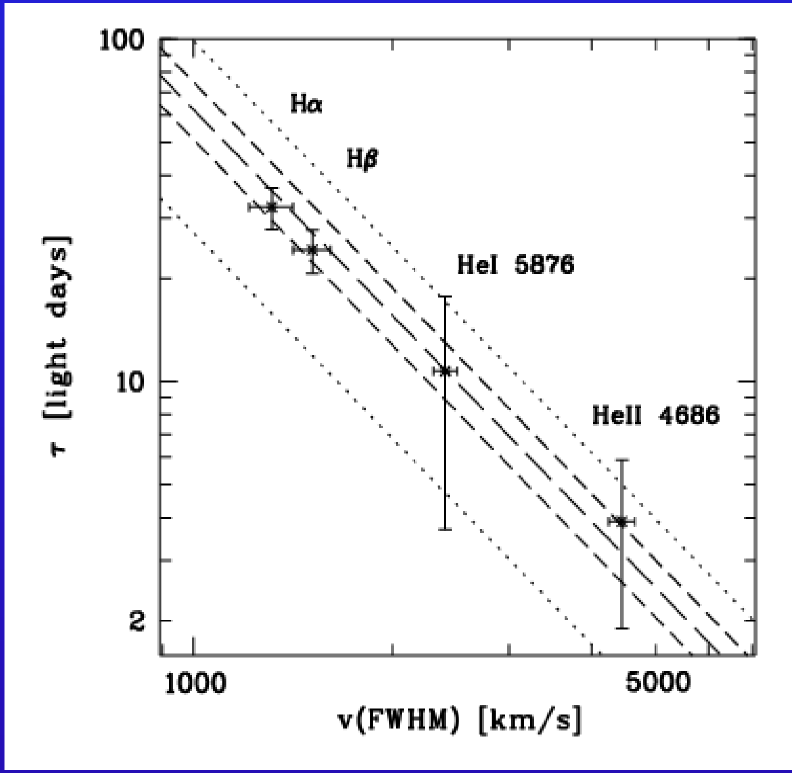

Mean distances of the line emitting regions from central ionizing source as function of FWHM in rms profiles.

The rms spectrum shows the variable part of the spectrum

The dotted and dashed lines correspond to virial masses of .8 - 2.9 $10^7 M_O$ (from bottom to top).

Central Black Hole Mass in Mrk110

Assumption:
emission line clouds are gravitationally bound by central object

$$M = \frac{f V_{\mathrm{FWHM}}^2 c\tau}{G}$$

cτ = mean dist. of line em. clouds

V = rot. vel. of clouds (from rms line width)

f = factor (½ - 5.5) (unknown geometry and kinematics)

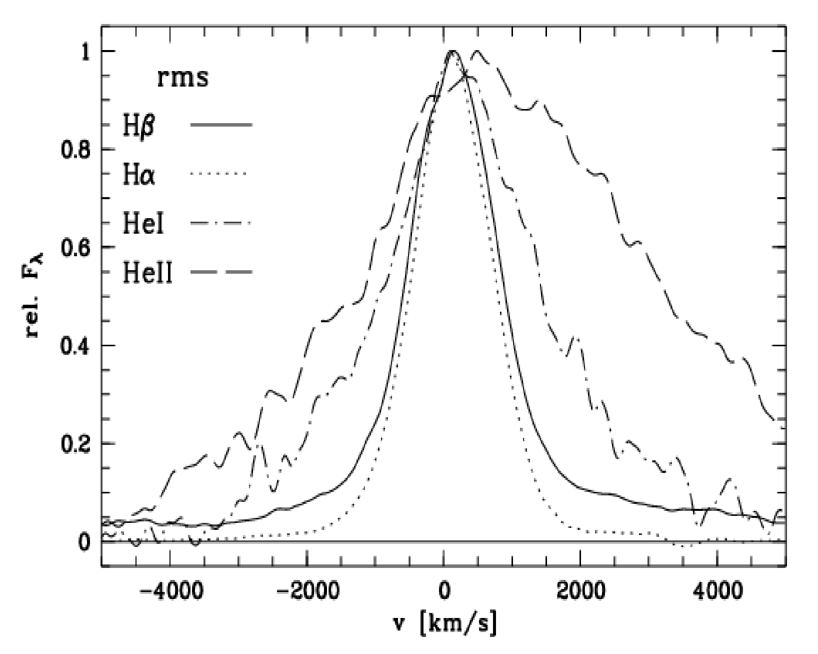

Normalized rms line profiles in velocity space

Line (1)	FWHM(rms) [km s^{-1}] (2)	τ_{cent} [days] (3)	M [$10^7 M_\odot$] (4)
HeIIλ4686	4444. ± 200	$3.5^{+2.}_{-2.}$	$2.25^{+1.63}_{-0.45}$
HeIλ5876	2404. ± 100	$10.8^{+4.}_{-4.}$	$1.81^{+1.36}_{-0.33}$
Hβ	1515. ± 100	$23.5^{+4.}_{-4.}$	$1.63^{+0.33}_{-0.31}$
Hα	1315. ± 100	$32.5^{+4.}_{-4.}$	$1.64^{+0.33}_{-0.35}$

Kollatschny et al., 2001, 2003

Central Black Hole Masses in AGN

Black hole mass vs. luminosity for AGN

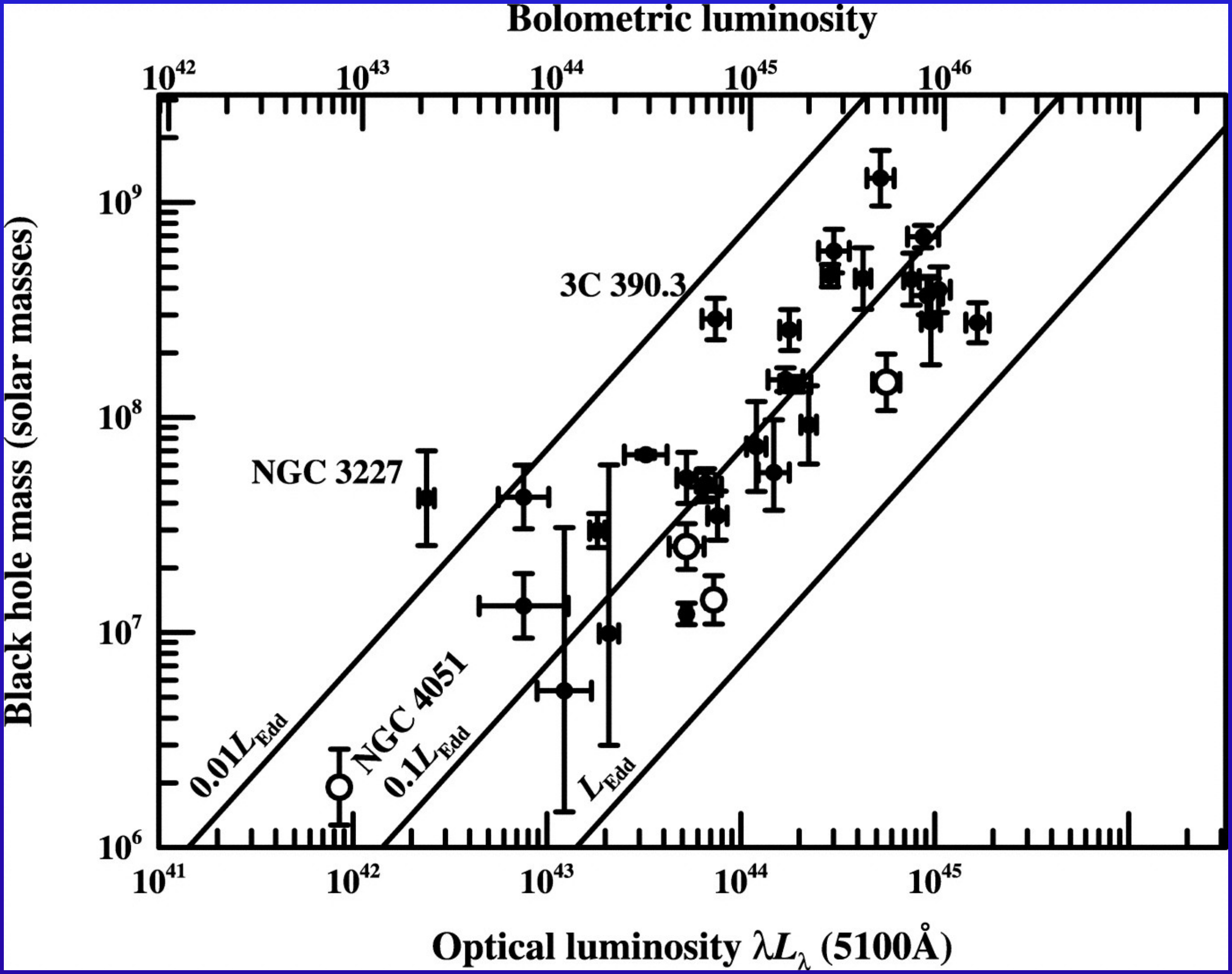

BH mass for 35 reverberation mapped AGN.

--- : lines of constant mass to luminosity ratio
open circles: NLSy1

Peterson et al., 2004

Balmer line averaged BLR size in AGN

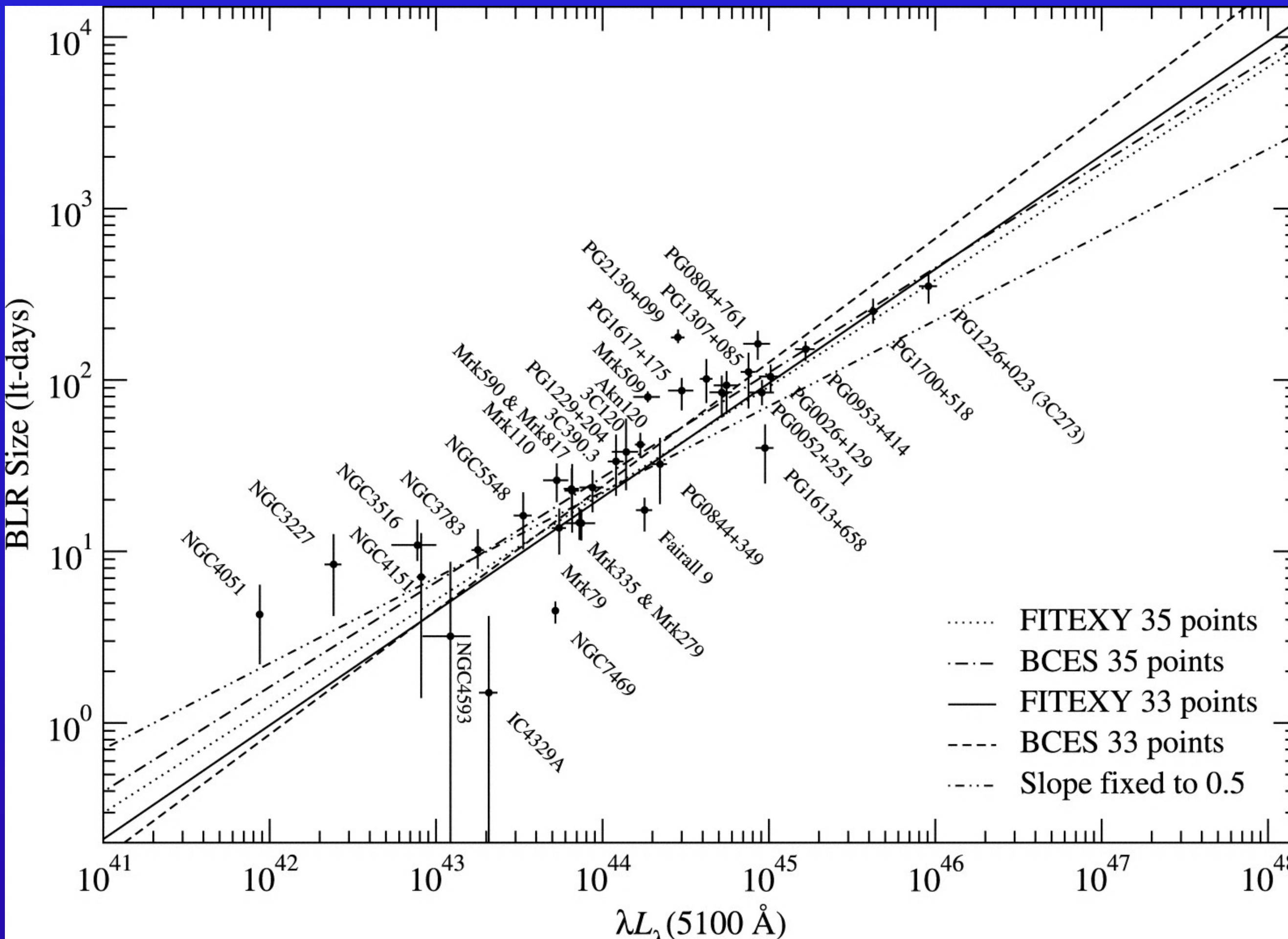

photoion. theory:

$$r = \left(\frac{Q(\mathrm{H})}{4\pi c n_\mathrm{e}} \right)^{1/2} \propto L^{1/2}$$

Q = hydrogen-ionizing photons emitted per sec

Relationship between luminosity and Hβ broad-line region size

$R_{BLR} \sim L^{0.65}$

But intrinsic scatter due to: BLR density, column density, ionizing spectral energy distribution, ...?

Kaspi et al. 2004

HET variability campaign of 3C120

Continuum light curve
(HET and Wise data)

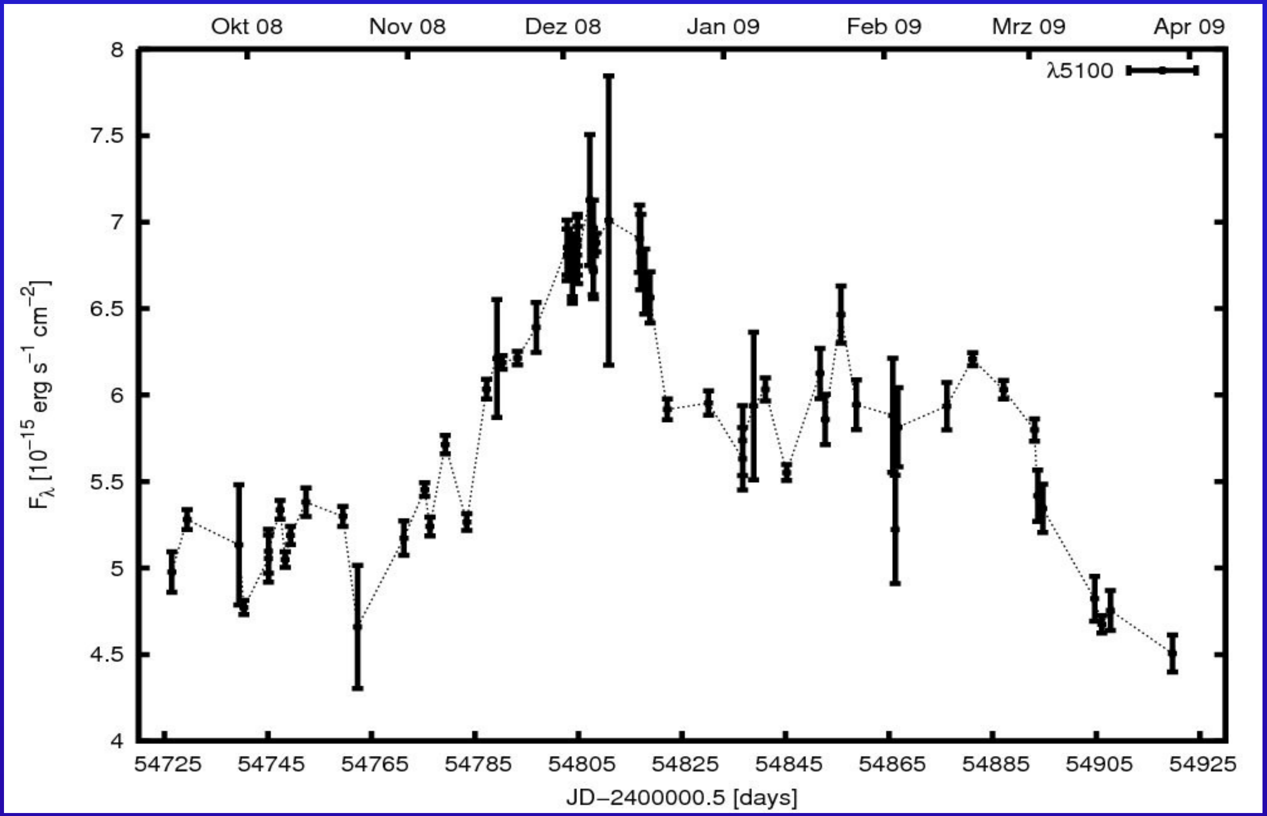

Sept. 2008 – Mar 2009

Kollatschny, Ulbrich, Kaspi, .. in prep

Variability and BLR structure in 3C120

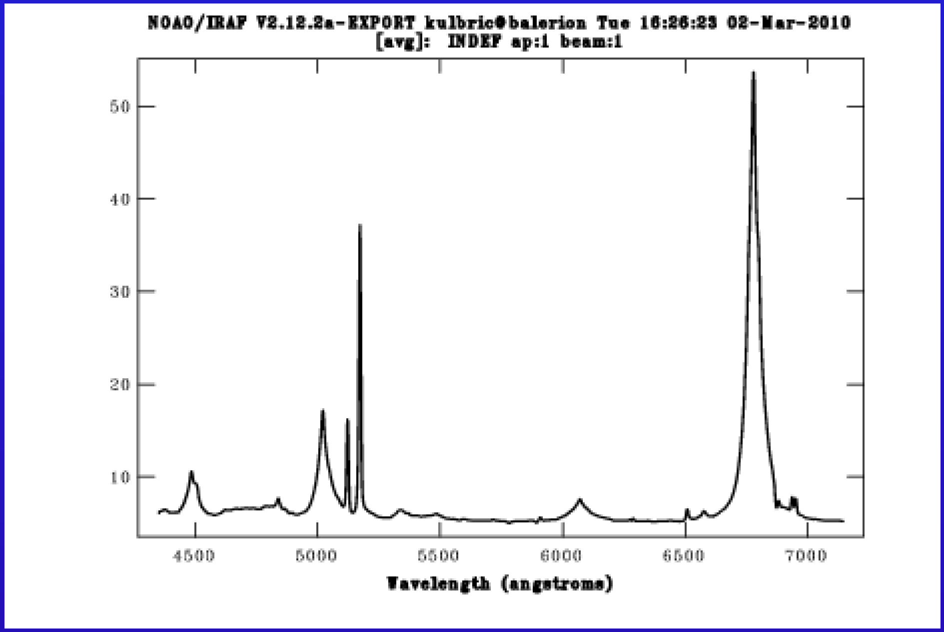

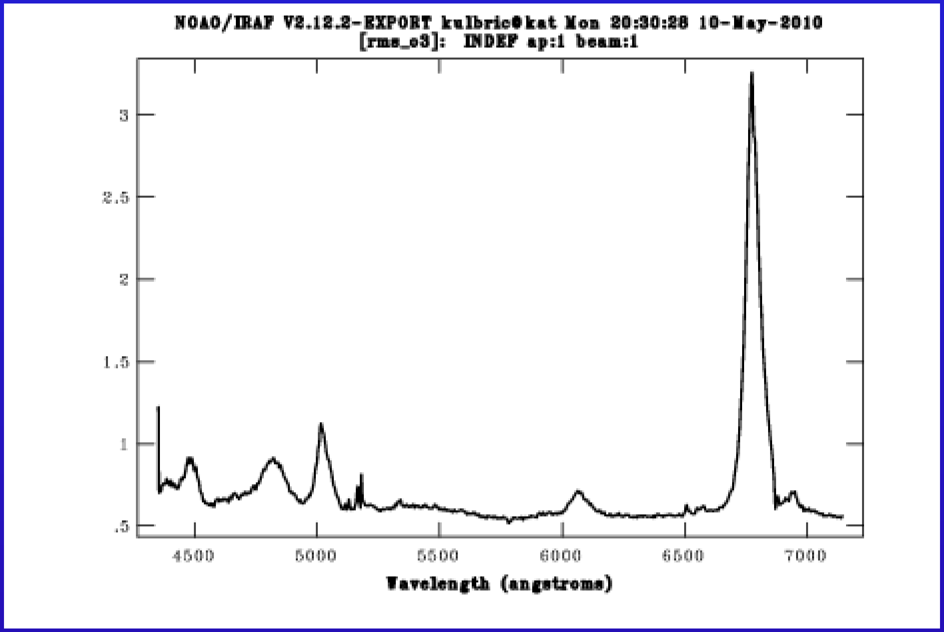

Mean spectrum of 3C120
for 31 epochs from Sept. 2008
through March 2009

Rms spectrum

Variability and BLR structure in 3C120

Continuum and integrated emission line (HeII, HeI, Hβ) light curves

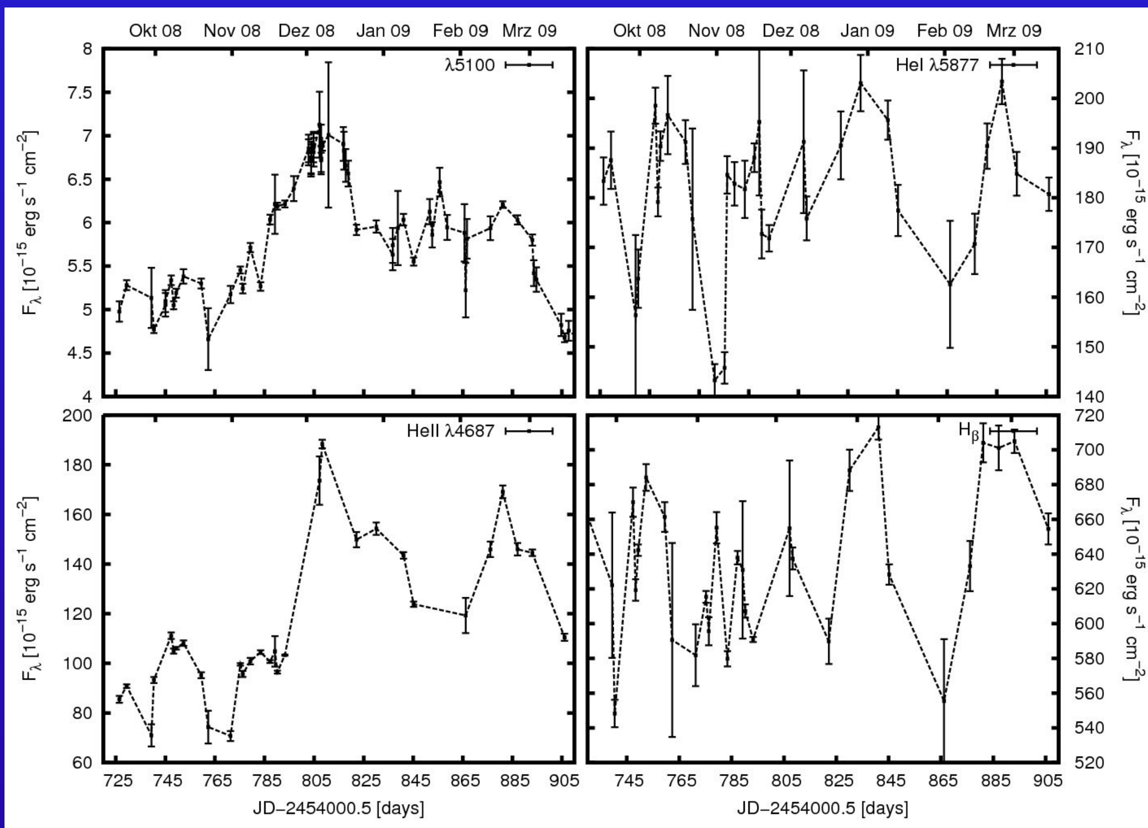

Sept. 2008 – Mar 2009

CCF functions of HeII and Hβ line light curves with continuum light curve

10.4 ± 3. *30.5 ± 3.*

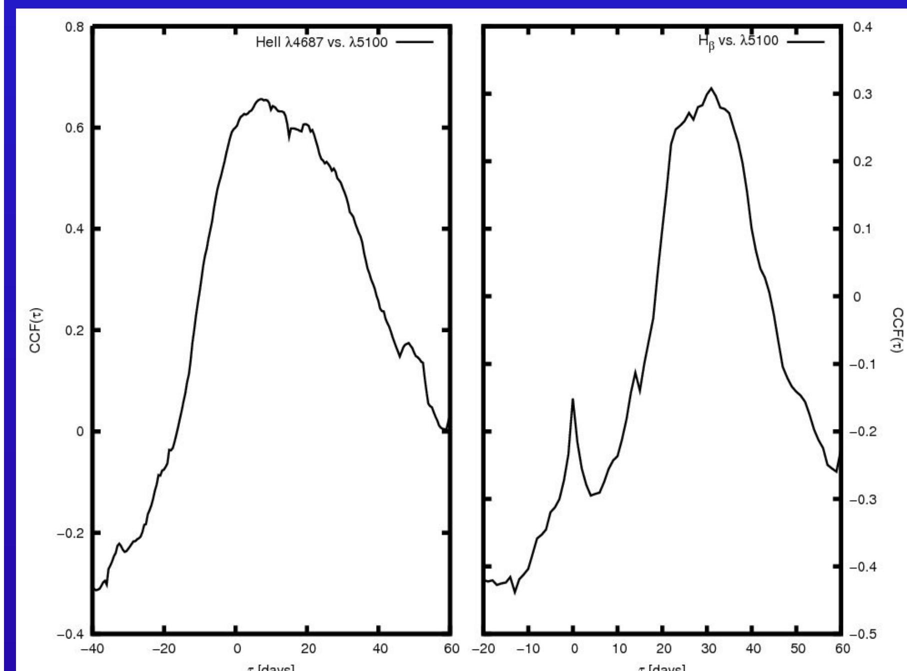

Delay in units of days

BLR size, stratification and BH mass in 3C120

Time lag (CCFs centroids) for various emission lines: HeII, HeI, Hγ, Hβ, Hα

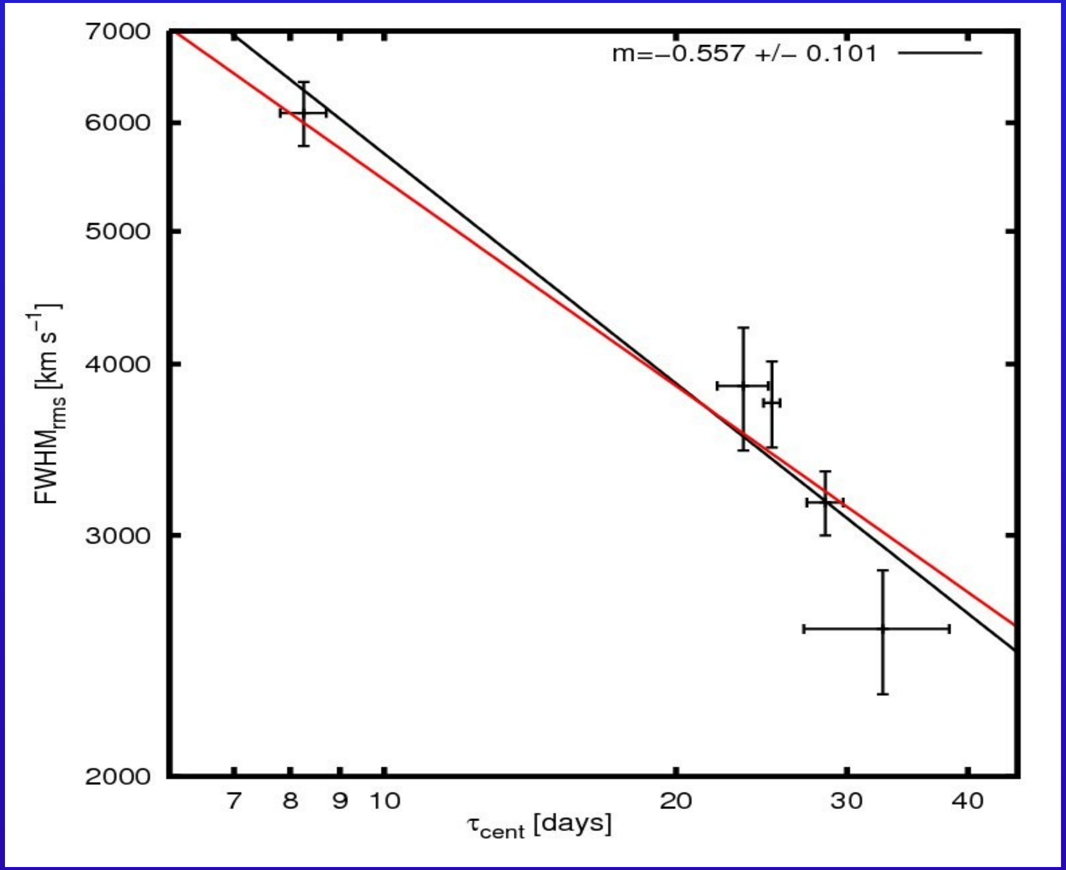

higher ionized lines: - broader line widths
- faster response

$$M = \frac{f V^2_{\mathrm{FWHM}} c\tau}{G}$$

Line	BH mass $[10^7 M_{solar}]$
Hα	5.6 ± 1.5
Hβ	7.5 ± 0.9
Hγ	9.2 ± 1.3
HeI	9.1 ± 1.9
HeII	8.0 ± 0.9
Mean	7.9 ± 1.5

Study of Variability, Study of Line Profiles

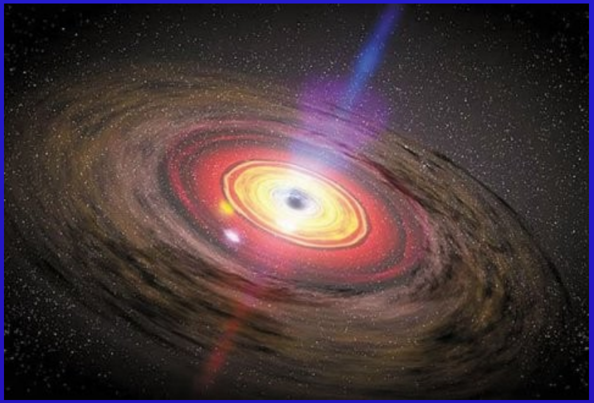

2) Study of line profile variability

- Geometry and Kinematics in the BLR

- *central Black Hole Mass*

in Mrk110, 3C390.3

BLR Kinematics: Idealized Model

Influence of BLR motions on line profile variations

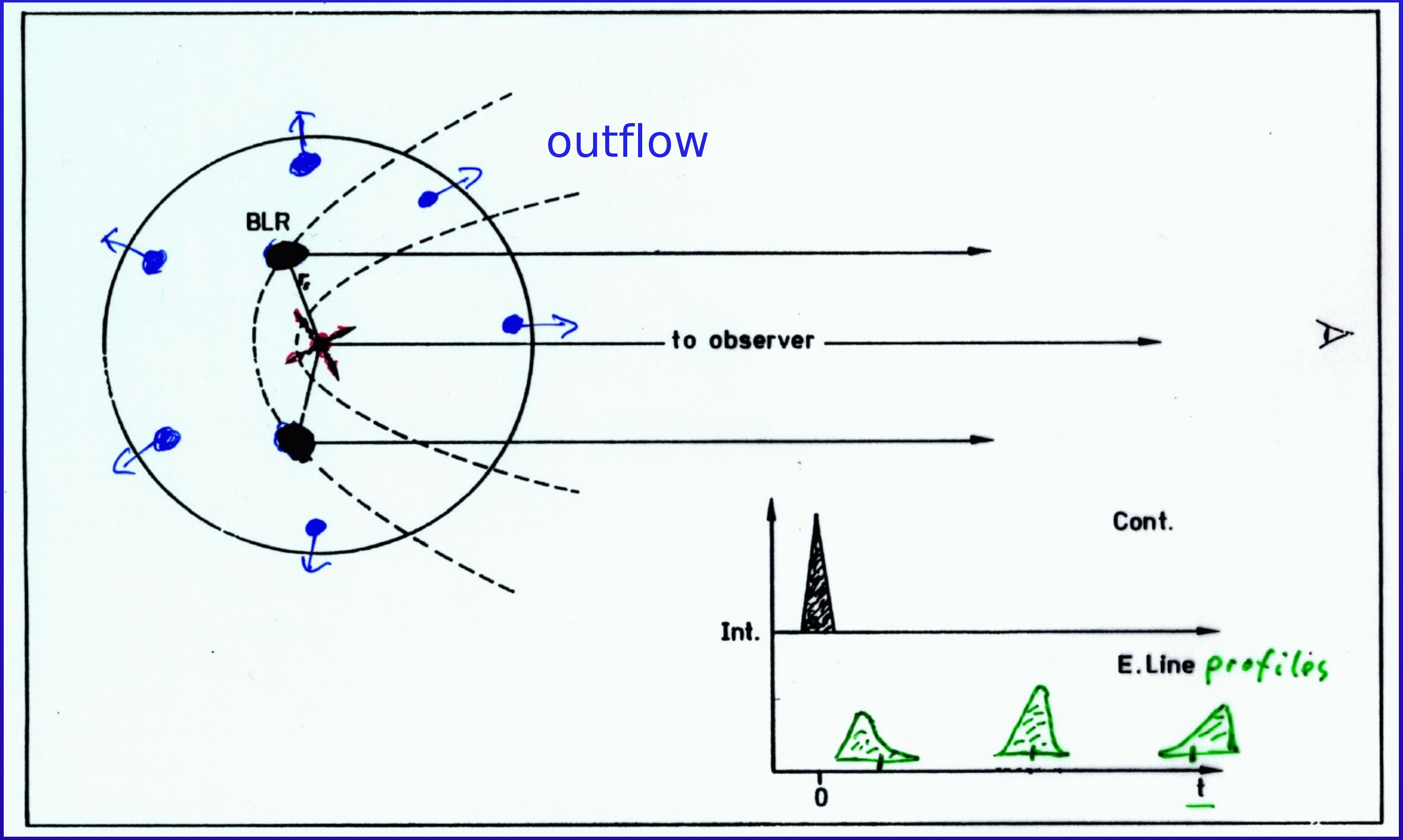

Theory : BLR kinematics - line profile variations

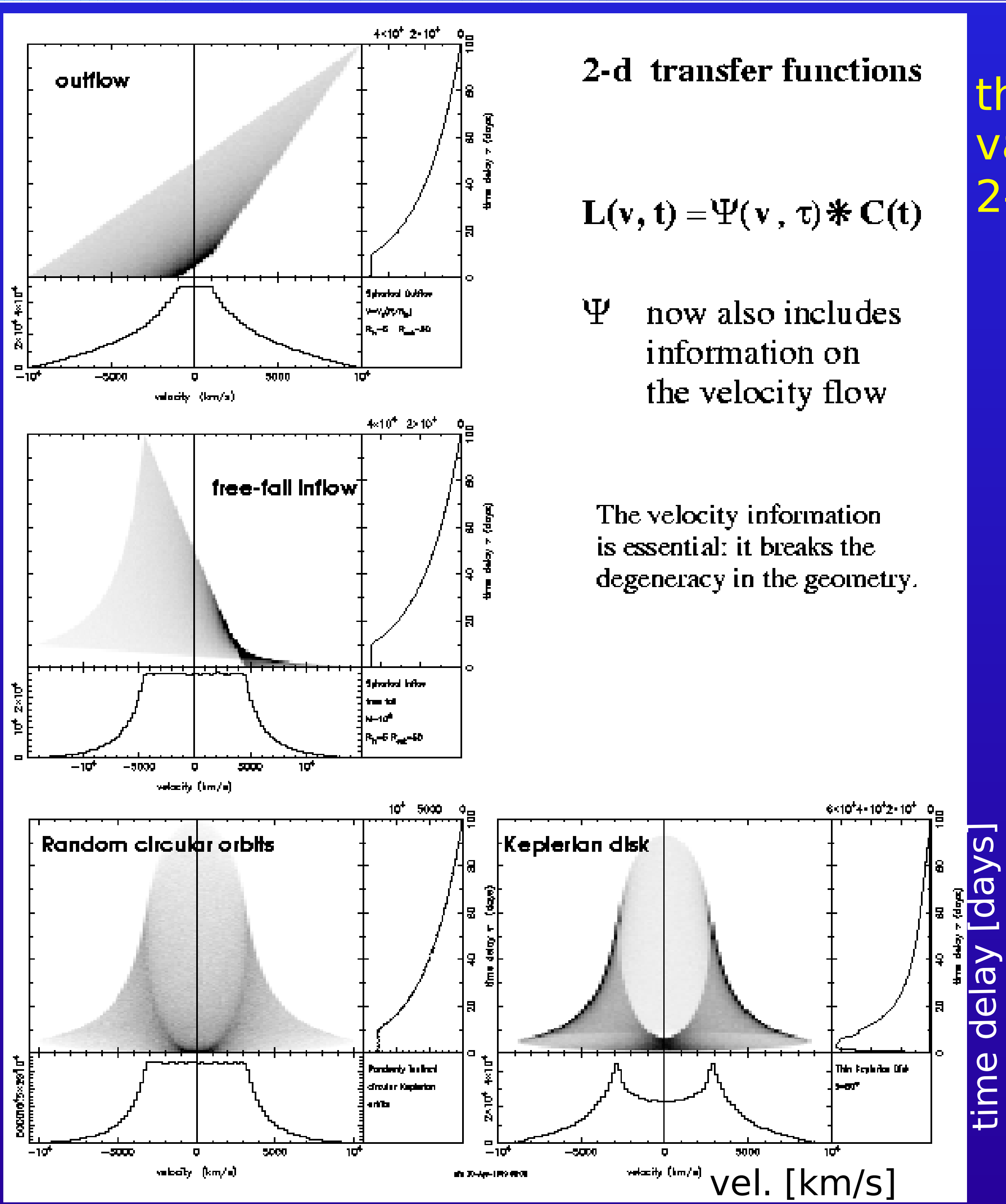

theoretical emission line profile variations to derive 2-dim. velocity-delay maps Ψ

velocity-delay maps for different flows

Welsh & Horne, 1991

Horne et al., 2004

BLR kinematics and accretion disk structure

Mean Hβ line profile of Mrk110 in velocity space

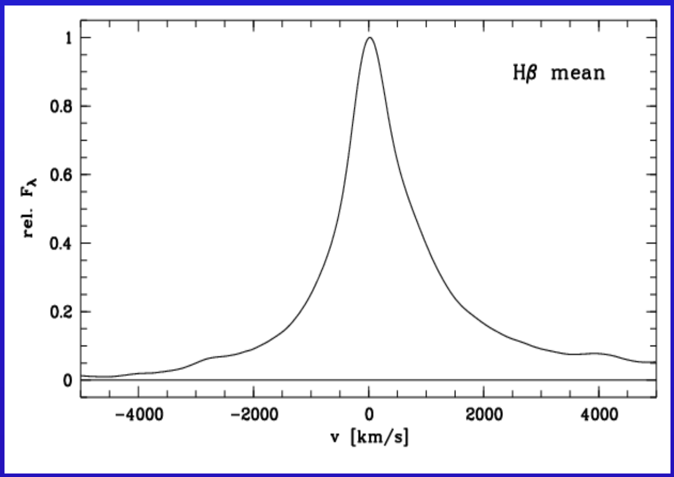

Light curves of the continuum, of the Hβ line center, and of different blue and red line wing segments

Δv = 400 km/s

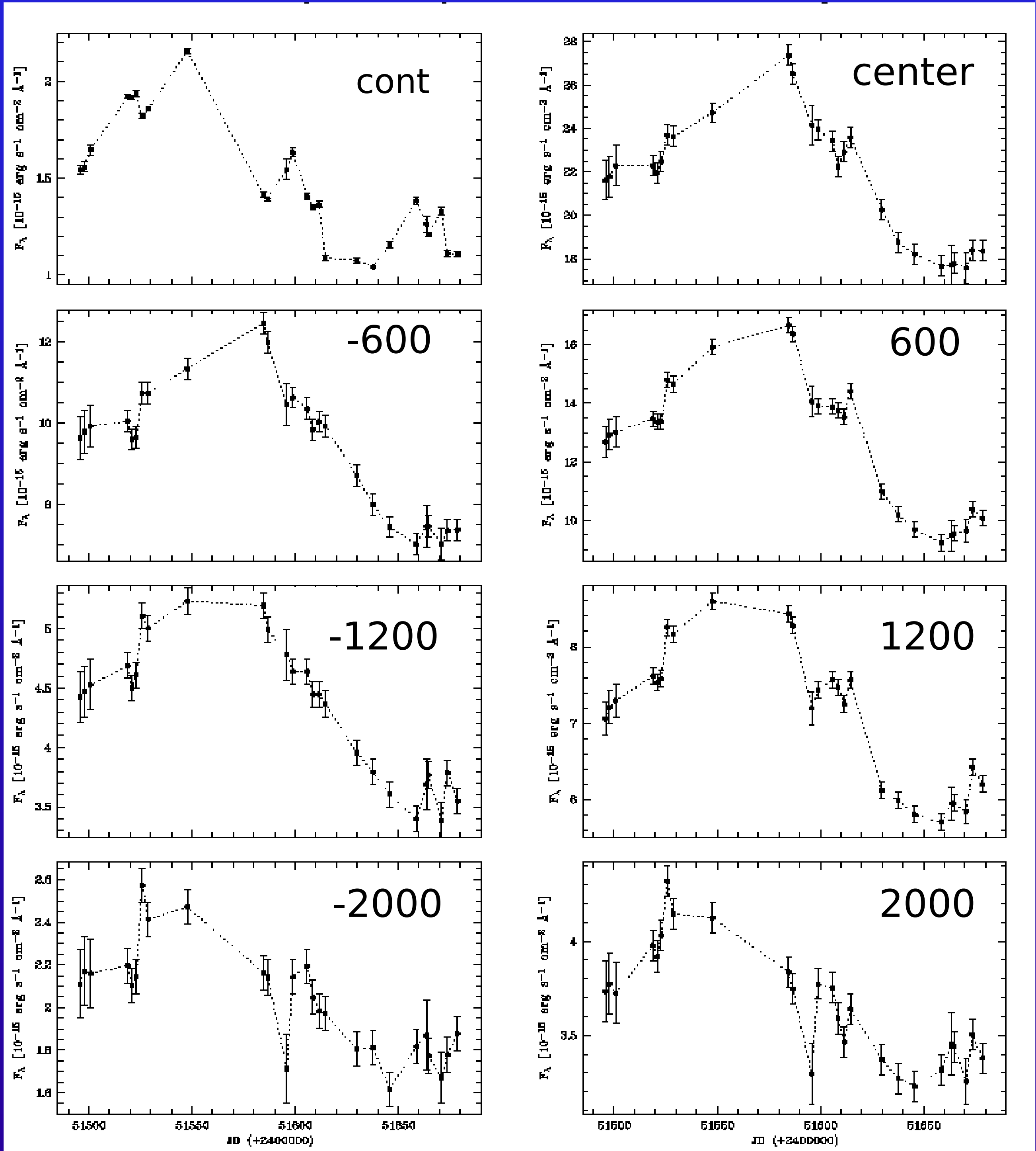

Kollatschny & Bischoff 2002

BLR: Accretion disk structure in Mrk110

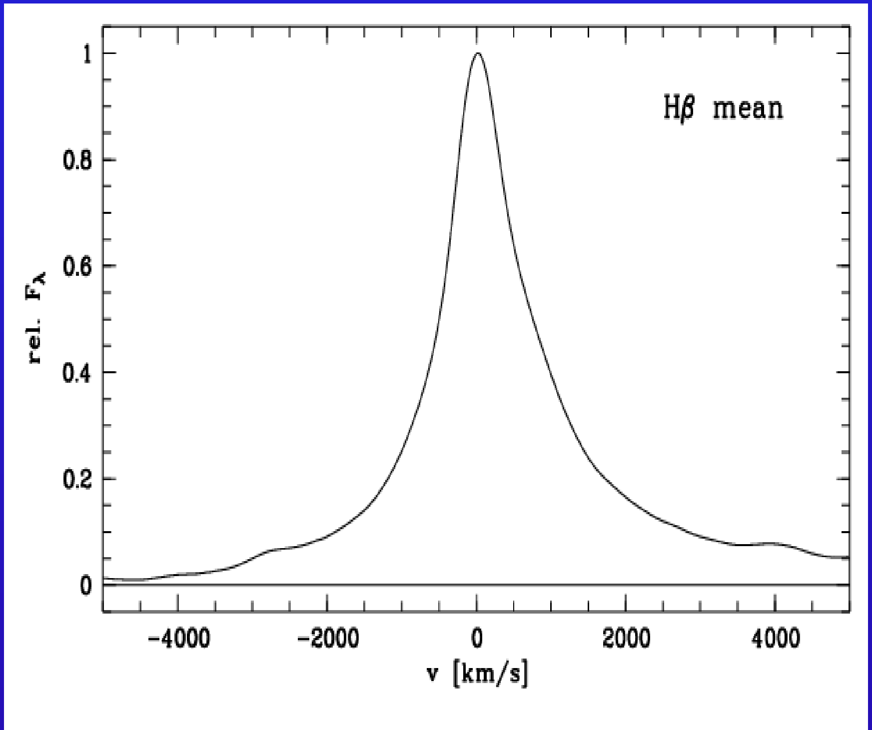

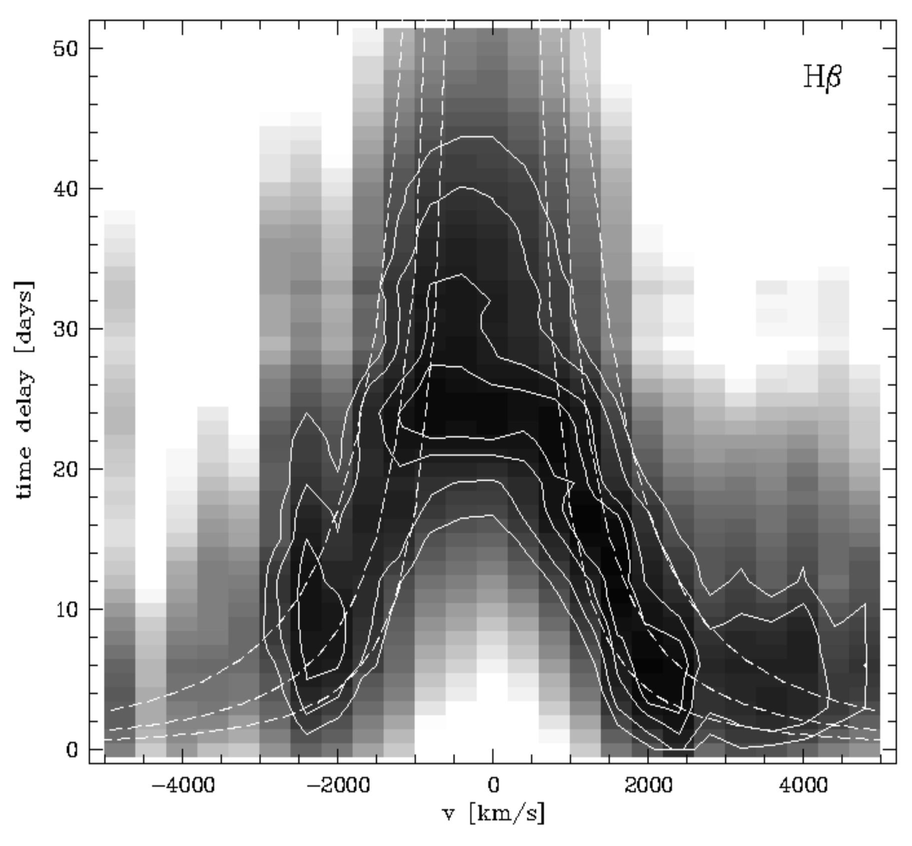

Mean Hβ line profile of Mrk110 in velocity space

Velocity-delay map

Kollatschny 2003a

BLR: Accretion disk structure in Mrk110

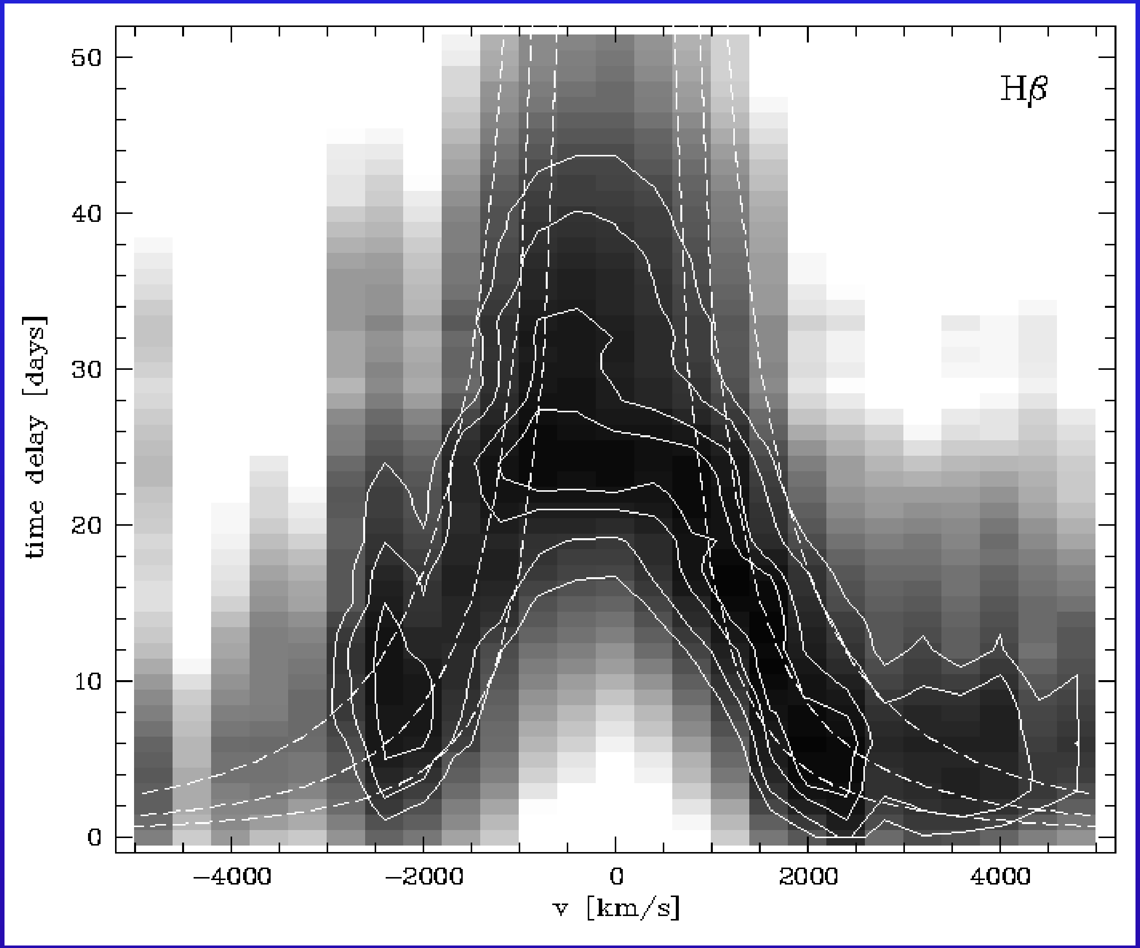

Velocity-delay map

Kollatschny 2003a

2-D CCF : correlation of Hβ line profile segments with cont. variations (grey scale)

Contours of correlation coefficient at levels of .85 to .925 (solid lines).

Dashed curves: theoretical escape velocity envelopes for masses of 0.5, 1., 2. 10^7 M_o (from bottom to top).

Echo image

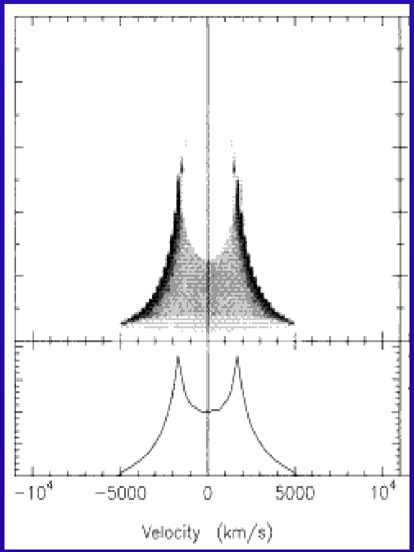

Theoretical velocity-delay maps for different flows: Keplerian disk BLR model: fast response of both outer line wings

Welsh & Horne 1991, Horne et al. 2004

Velocity-delay maps: accretion disk structure

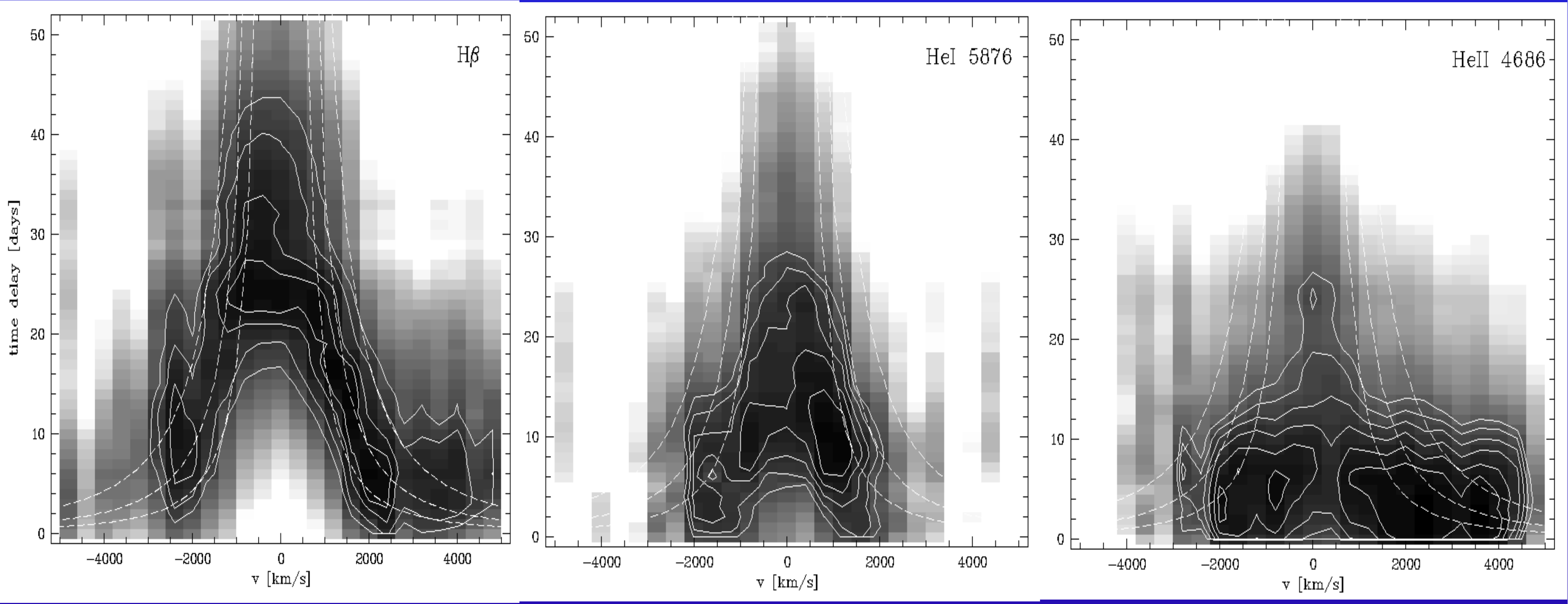

2-D CCF : correlation of Hβ, HeI, HeII line profile segments with continuum variations (grey scale).

Kollatschny 2003

Keplerian disk BLR model: fast response of both outer line wings

Solid line: innermost radius at 5 ld

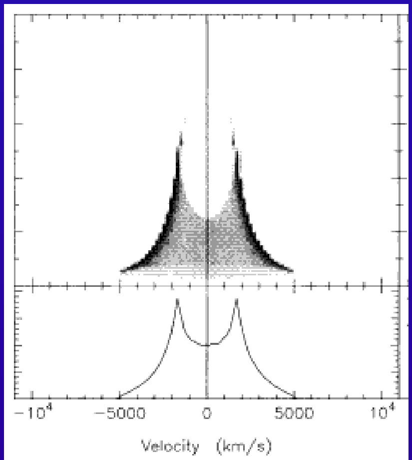

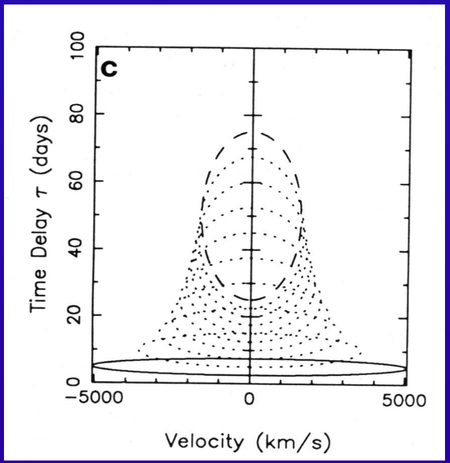

BLR: Accretion disk wind in Mrk110

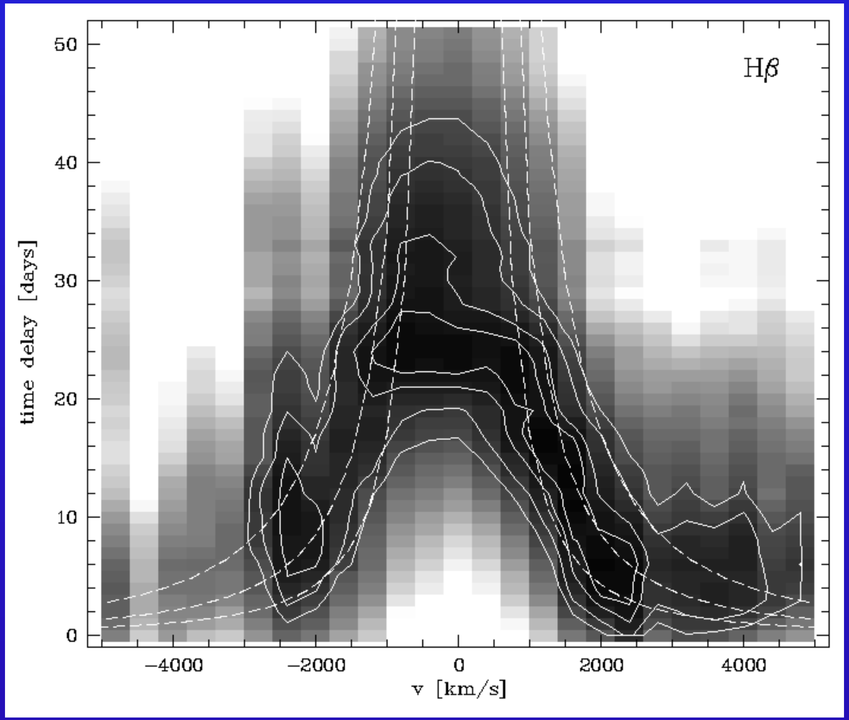

2-D CCF: velocity-delay map

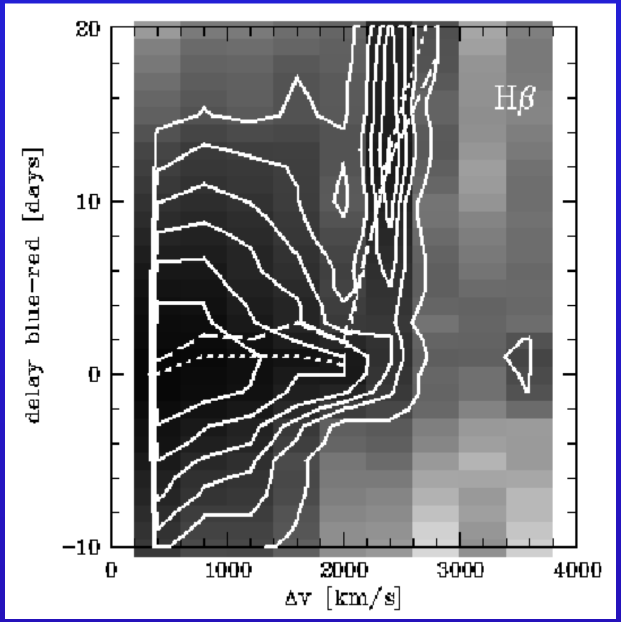

Time delay of blue line wing to red line wing as function of dist. to line center

Outer line wings: inner BLR

Disk wind model of BLR: Slightly faster and stronger resonse of red wing

Chiang & Murray, 1996

Disk driven outflow models compared to spherical wind models: velocity decreases with radius (rather than the other way around)

Koenigl & Kartje, 1994

BLR Structure and Kinematics in Mrk110

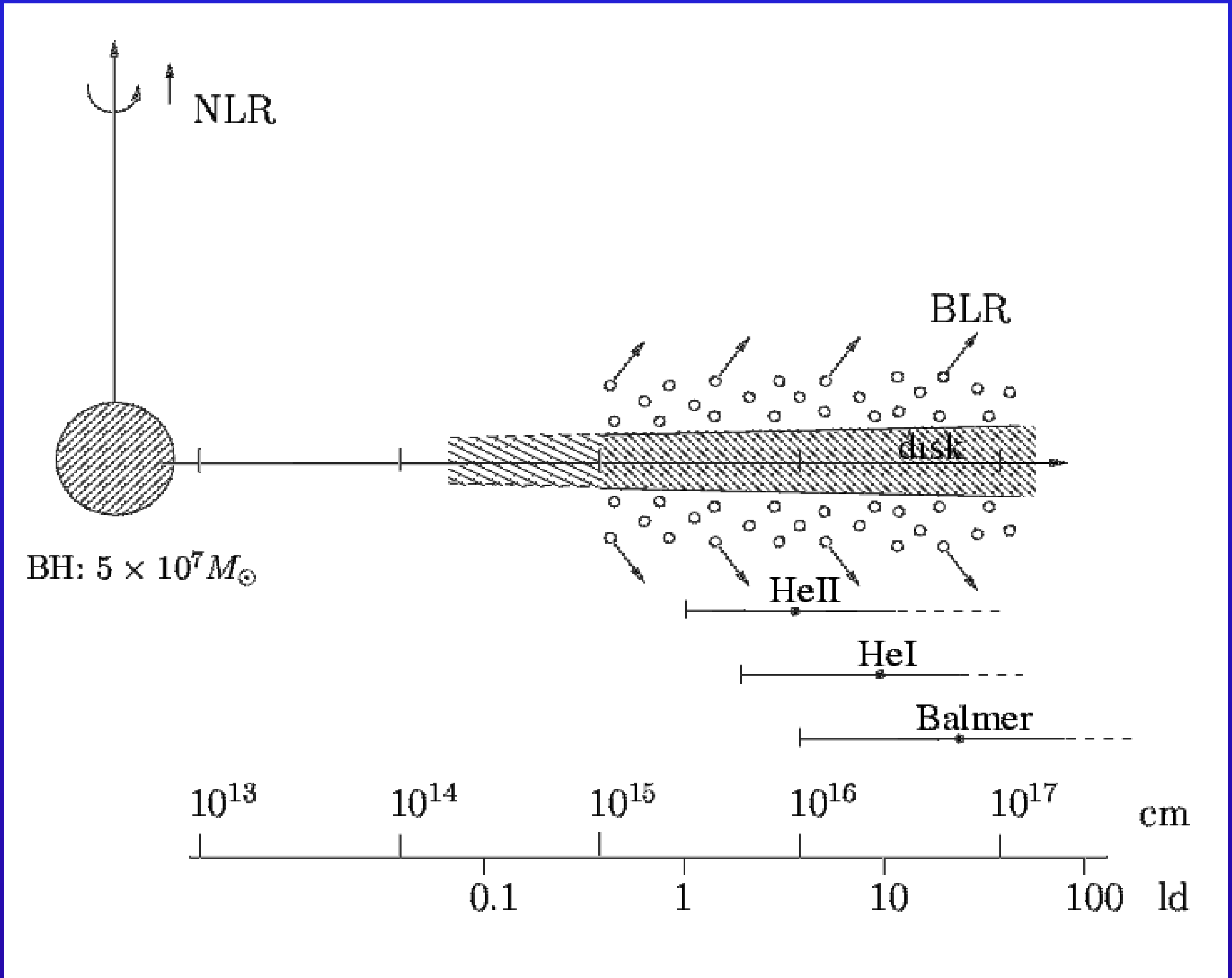

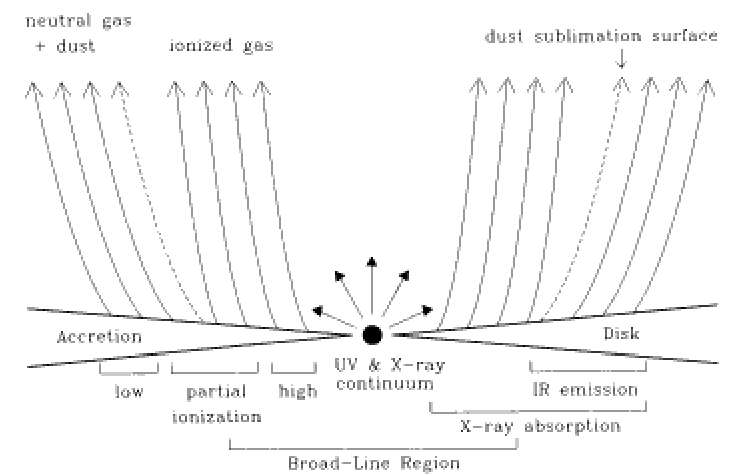

FIG. 13.—Schematic representation of how a disk-driven hydromagnetic wind, which is characterized by a highly stratified density distribution, interacts with the active galactic nucleus (AGN) continuum emission. The innermost regions are heated and ionized by the powerful radiation field, with the temperature and degree of ionization varying both with distance and with the polar angle, whereas the outer regions (beyond the dust sublimation radius) are cooler and contain dust. The radiation pressure force on the dust causes the outer streamlines to have a larger opening angle.

Koenigl & Kartje 1994

accretion disk wind in Mrk110

Kollatschny 2003a

BLR: Accretion disk structure in 3C390.3

Information about accretion disk structure in 3C390.3 from shape of line profiles

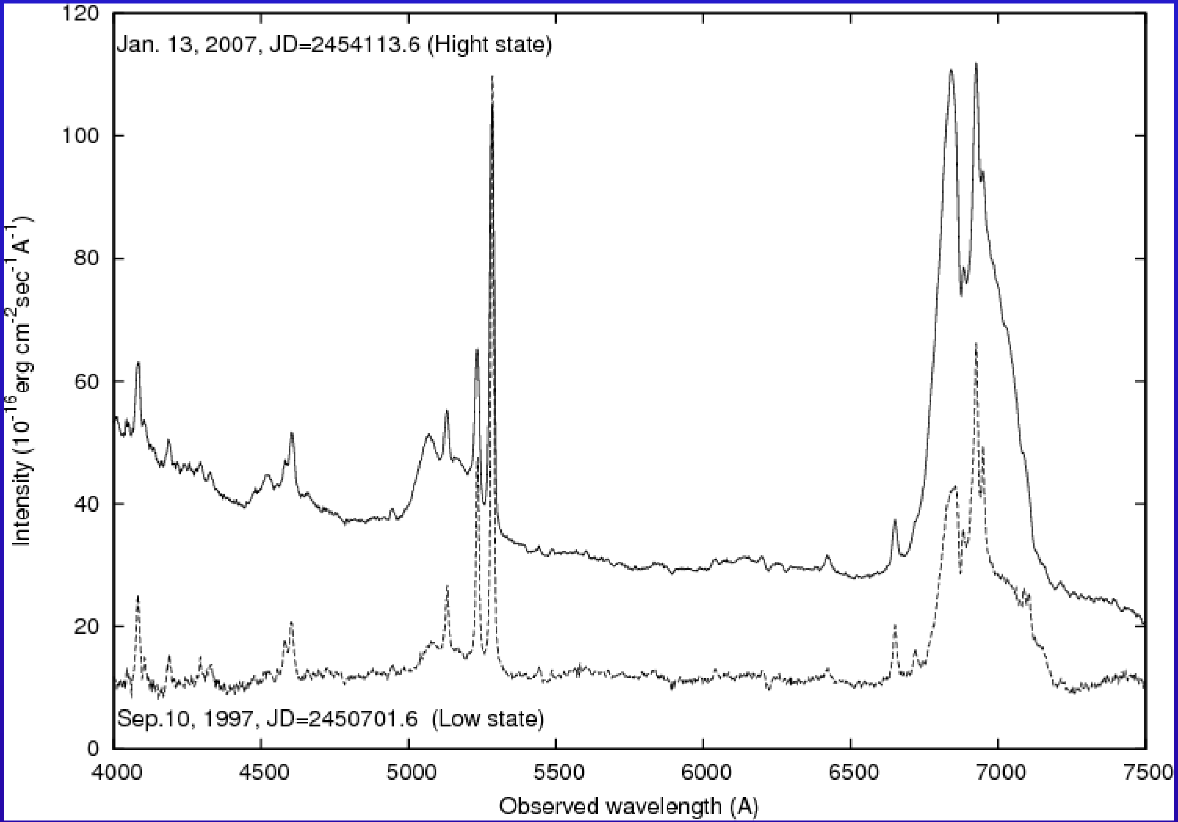

Spectra of 3C390.3 close to maximum (2007) and minimum (1997)

Shapovalova et al. 2010, Popovic et al. 2011

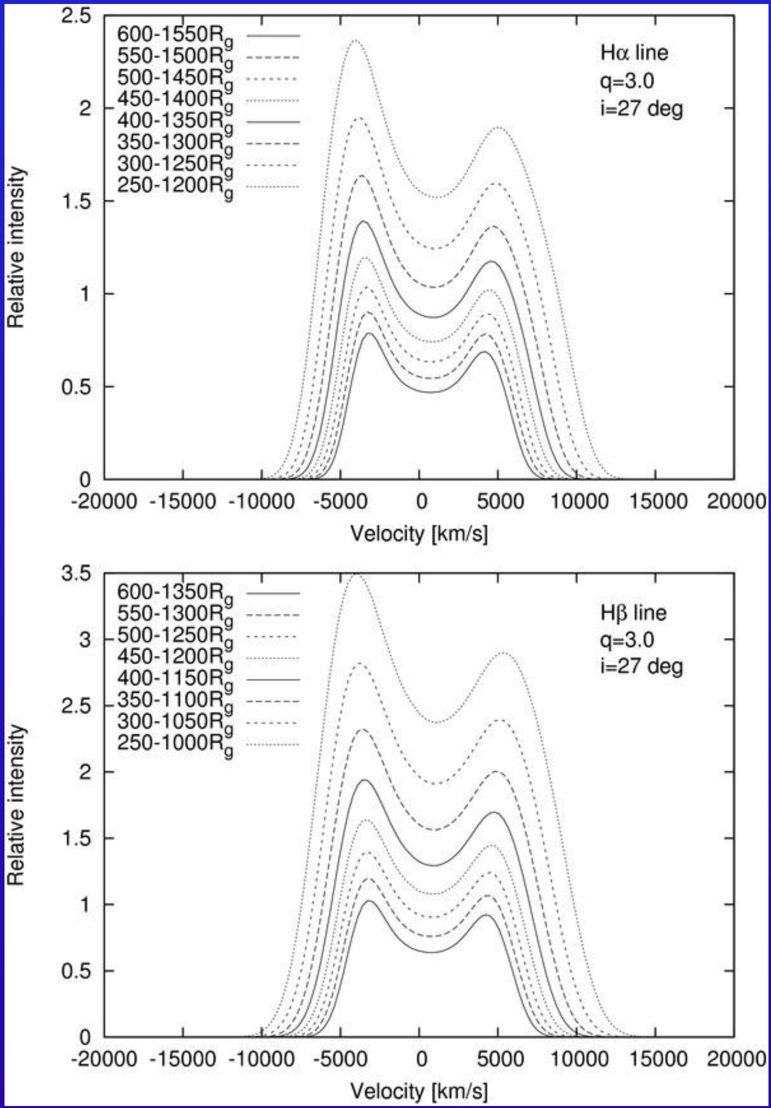

Modeled Hα ,Hβ line profiles for different disk parameters

BLR: Accretion disk structure in 3C390.3

Information about accretion disk structure in 3C390.3 also from line profile variations

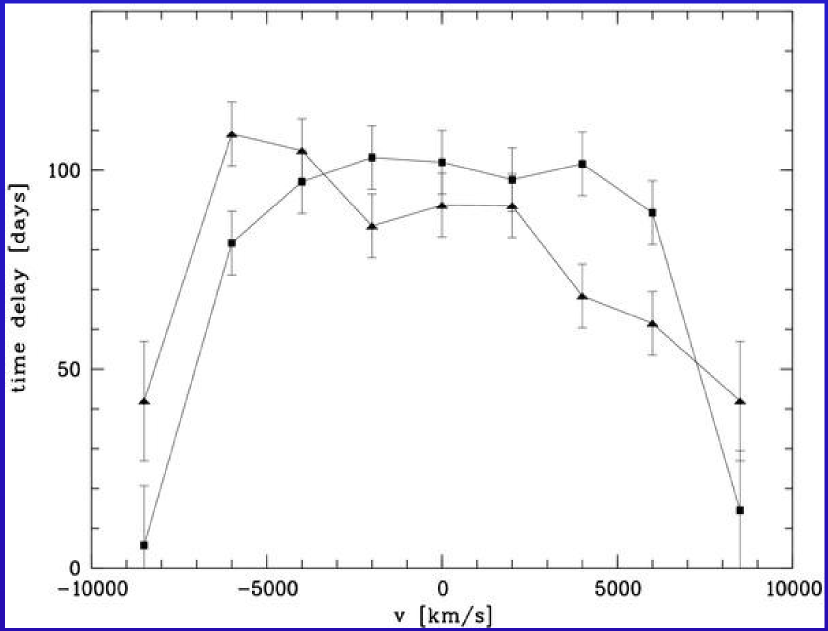

Time delay of individual Hβ line segments with respect to continuum light curve (1995-2002: squares, 2003-2007: triangles)

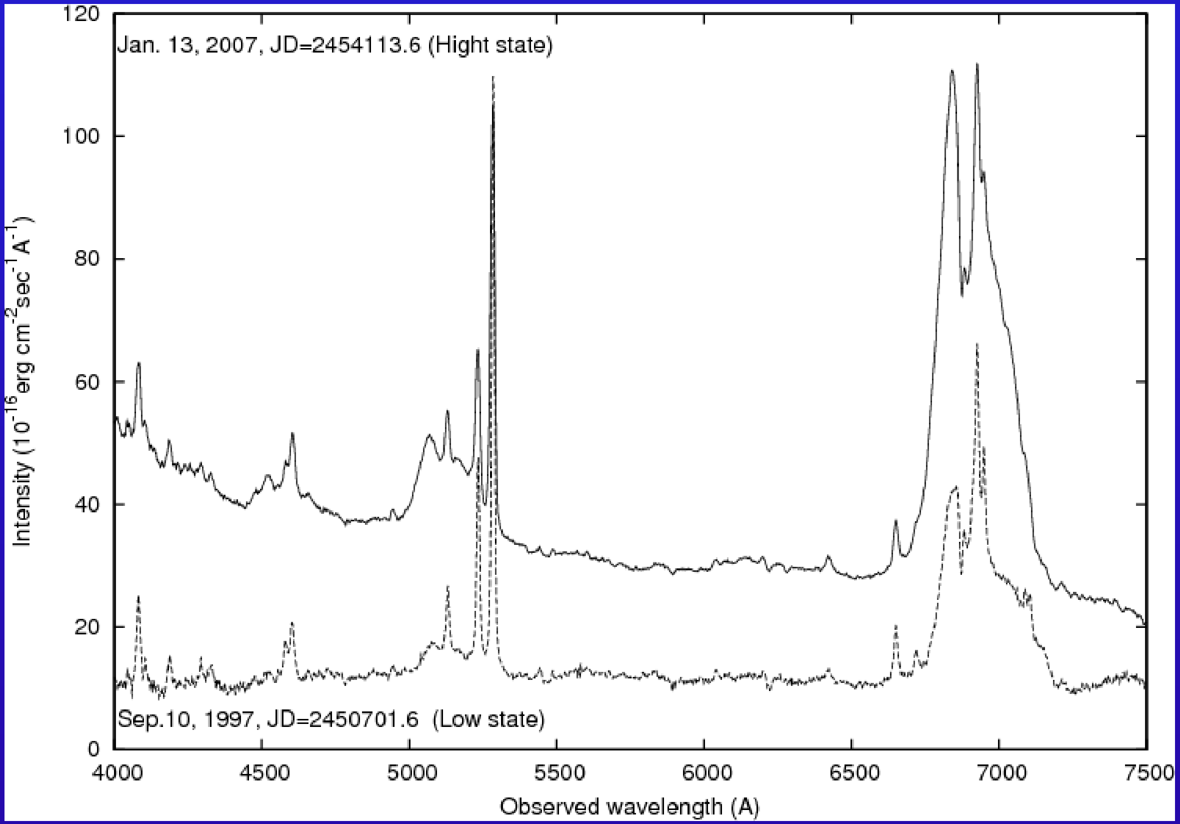

Spectra of 3C390.3 close to maximum (2007) and minimum (1997)

Shapovalova et al. 2010, Popovic et al. 2011

Study of Variability, Study of Line Profiles

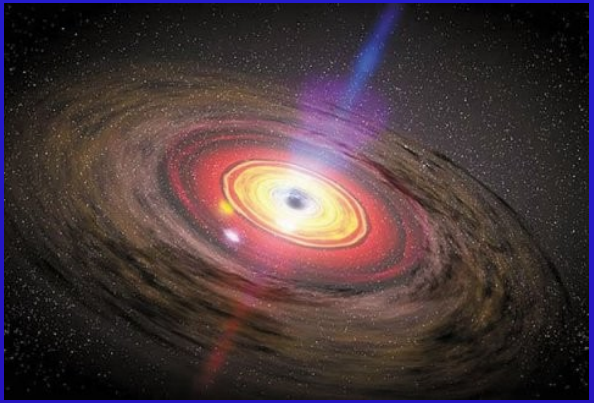

3) Study of general trends in line profiles

- Geometry and Kinematics in the BLR

- *central Black Hole Mass*

In AGN sample

Line profile studies: BLR structure & kinematics

Black hole mass estimations based on BLR kinematics – derived from line-width measurements (FWHM, line dispersion σ) of the mean or rms line profiles of Hβ

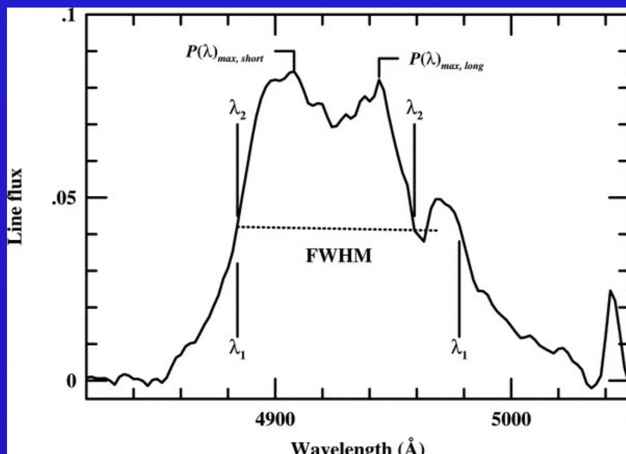

Line dispersion.—The first moment of the line profile is

$$\lambda_0 = \int \lambda P(\lambda) d\lambda \Big/ \int P(\lambda) d\lambda. \quad (4)$$

We use the second moment of the profile to define the variance or mean square dispersion

$$\sigma^2_{\rm line}(\lambda) = \langle \lambda^2 \rangle - \lambda_0^2 = \left[\int \lambda^2 P(\lambda) d\lambda \Big/ \int P(\lambda) d\lambda \right] - \lambda_0^2. \quad (5)$$

The square root of this equation is the line dispersion $\sigma_{\rm line}$ or rms width of the line.

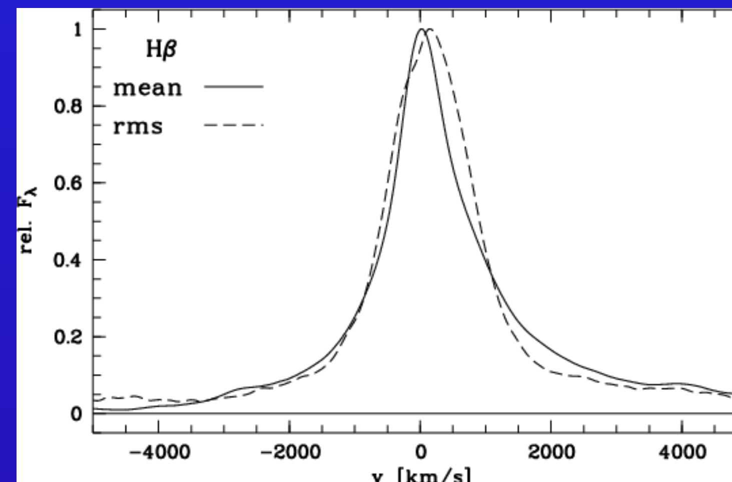

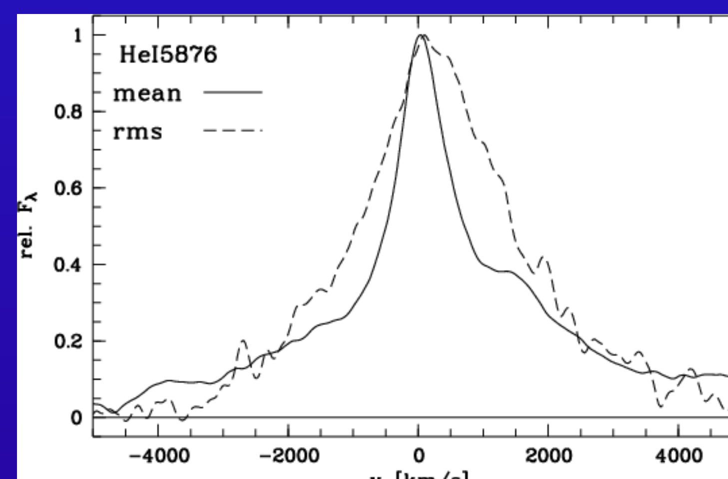

Peterson et al., 2004

Mrk110 Kollatschny, 2003

Hβ line-width ratio FWHM/σ versus σ

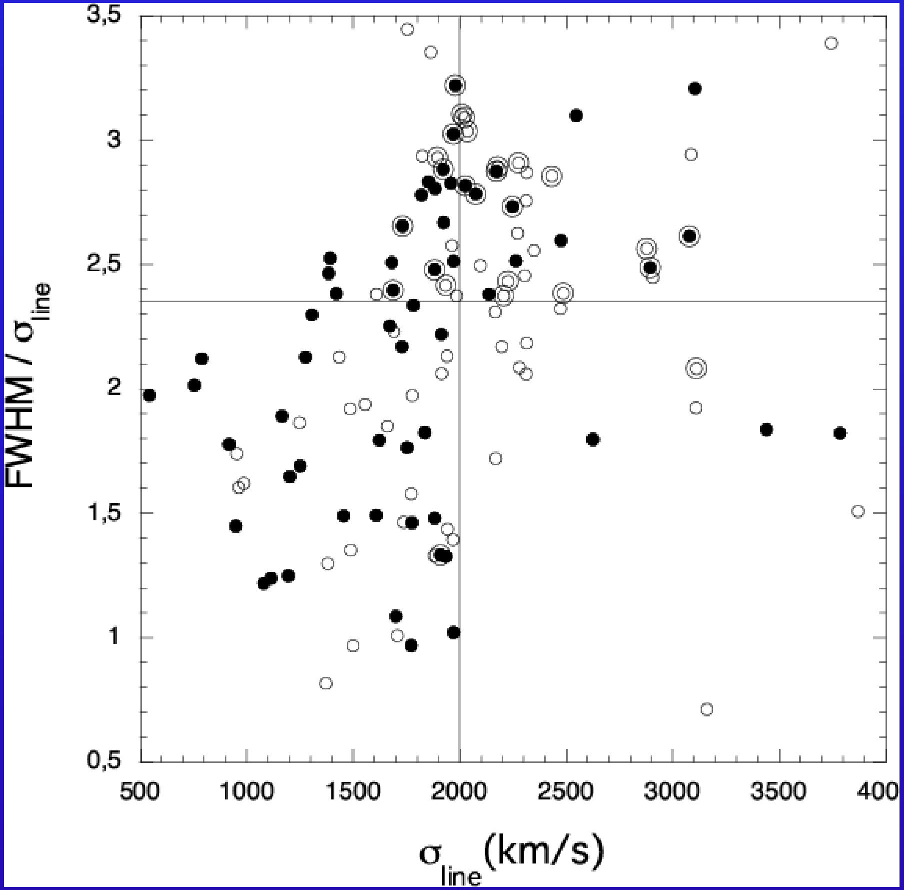

Data set (35 AGN) Peterson, 2004

Relationship between FWHM and σ depends on the line profile:

	FWHM/σ
- rectangular fct.	3.46
- edge-on rotat. ring	2.83
- triangular fct.	2.45
- Gaussian profile	2.35
- Lorentzian profile	→ 0.

Collin et al., 2006

Open and filled circles correspond to values based on mean and rms spectra.

The vertical line at σ = 2000 km/s approximates the division of Sulentic et al. (2000) into Populations A (left) and B (right).

The horizontal line at 2.35 divides the samples into Populations 1 (lower) and 2 (upper) (Collin et al., 2006).

Line-width ratios FWHM/σ for different line profiles

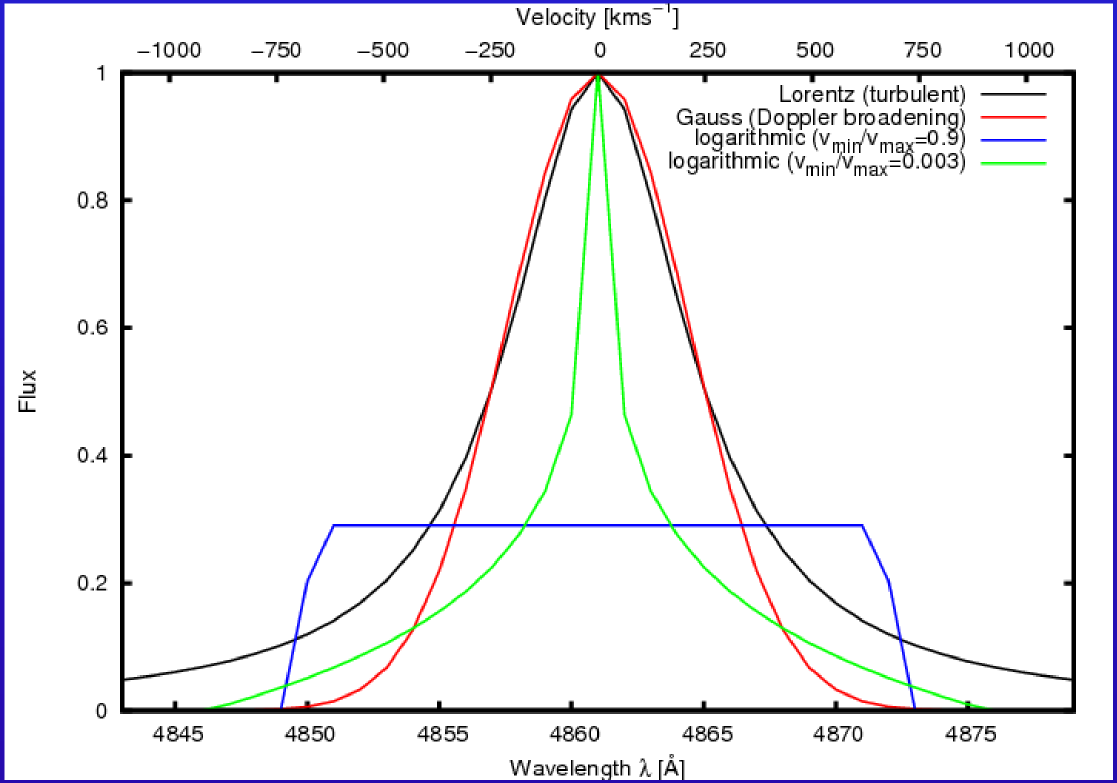

Relationship between FWHM and σ depends on the line profile:

	FWHM/σ
- rectangular fct.	3.46
- edge-on rotat. ring	2.83
- Gaussian profile	2.35
- logarithmic profile	→ 0.
- Lorentzian profile	→ 0.

Hβ line-width ratio FWHM/σ versus σ

Collin et al., 2006

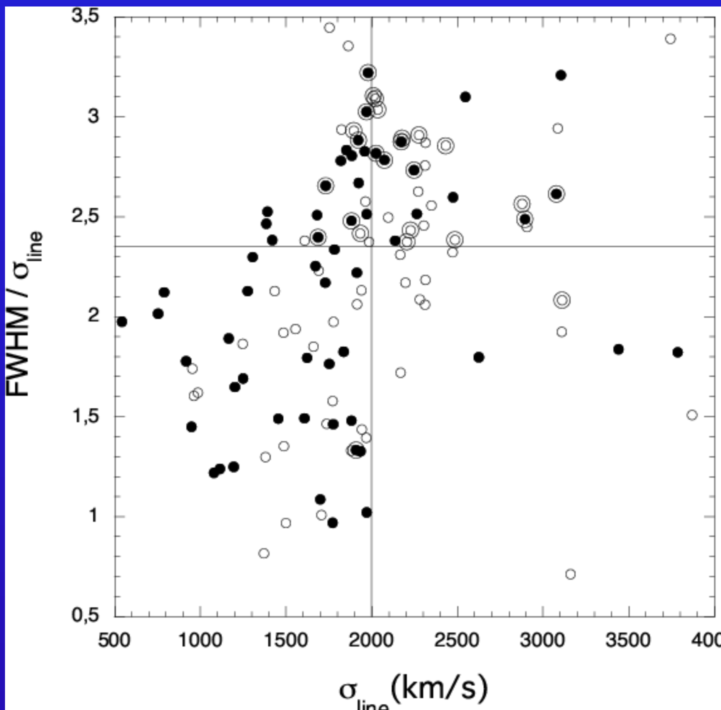

Kollatschny & Zetzl, 2011, Nature 470

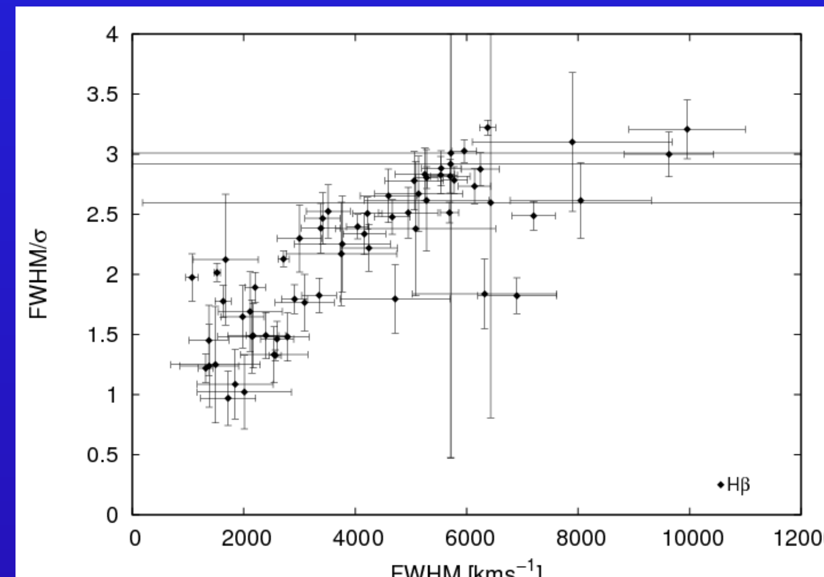

Hβ

The Hβ line-width ratio FWHM/σ versus σ (mean & rms profiles).

Table 1 | Line profile versus linewidth correlations

	r_p	r_s	r_k	P_p	P_s	P_k
Hβ FWHM/σ_{line} versus FWHM	0.792	0.823	0.649	6.4×10^{-15}	6.4×10^{-11}	3.5×10^{-14}
Hβ FWHM/σ_{line} versus σ_{line}	0.364	0.513	0.350	0.003	4.7×10^{-5}	4.4×10^{-5}
He II FWHM/σ_{line} versus FWHM	0.803	0.786	0.571	0.016	0.041	0.048
He II FWHM/σ_{line} versus σ_{line}	0.464	0.357	0.214	0.247	0.361	0.458
C IV FWHM/σ_{line} versus FWHM	0.821	0.821	0.619	0.023	0.049	0.051
C IV FWHM/σ_{line} versus σ_{line}	0.599	0.643	0.429	0.155	0.126	0.176

Given are the Pearson correlation coefficient r_p, the Spearman's rank-correlation coefficient r_s, as well as the Kendall correlation coefficient r_k for Hβ, He II $\lambda = 4{,}686$ Å and C IV $\lambda = 1{,}550$ Å linewidth ratios FWHM/σ_{line} versus FWHM as well as FWHM/σ_{line} versus σ_{line}. P_p, P_s and P_k are the associated percentage probabilities for random correlations[15,16]. The Pearson correlation coefficient tests a linear relation only, while the other correlation coefficients test for a general monotonic relation.

Kollatschny & Zetzl: The Hβ line-width ratio FWHM/σ versus FWHM (rms profiles)

HeII and CIV line-width ratios FWHM/σ versus FWHM

From Peterson (2004) data set:

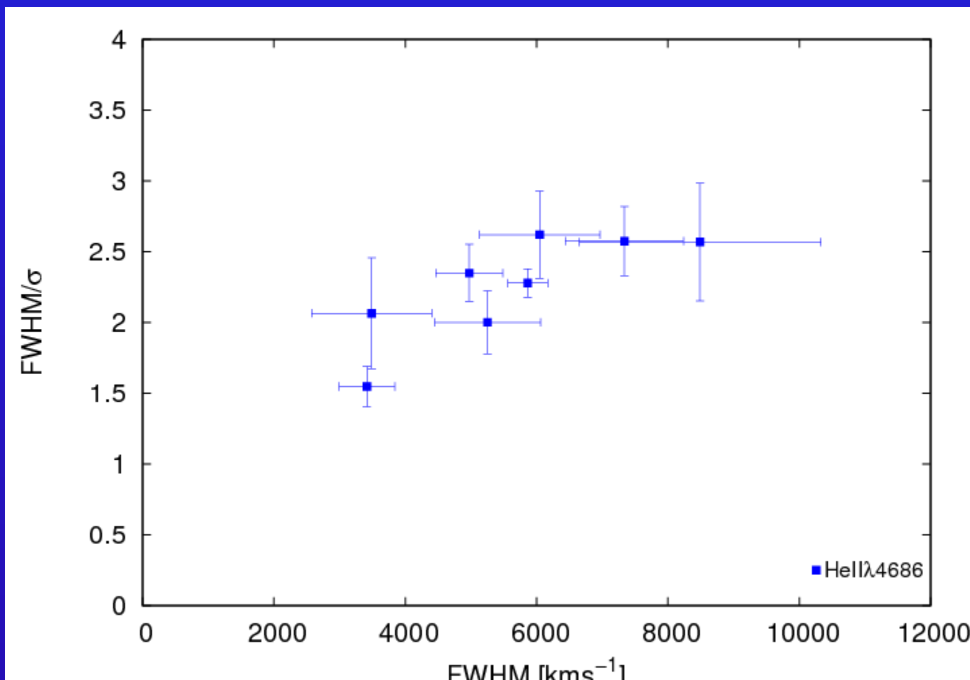

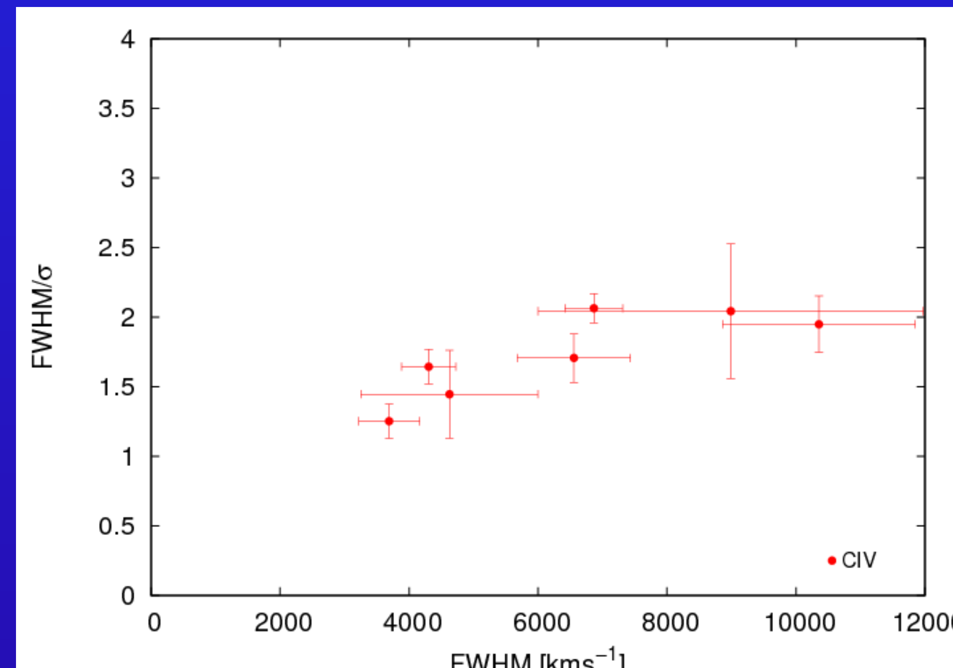

The HeIIλ4686 line-width ratio FWHM/σ versus FWHM (rms profiles).

The CIVλ1549 line-width ratio FWHM/σ versus FWHM (rms profiles).

Kollatschny & Zetzl, 2011, Nature 470

Different emission lines show similar – however different – systematics in the line profile relations.

Line profile studies: BLR structure & kinematics

Observed Hβ, HeII and CIV line-width ratios FWHM/σ versus linewidth FWHM.

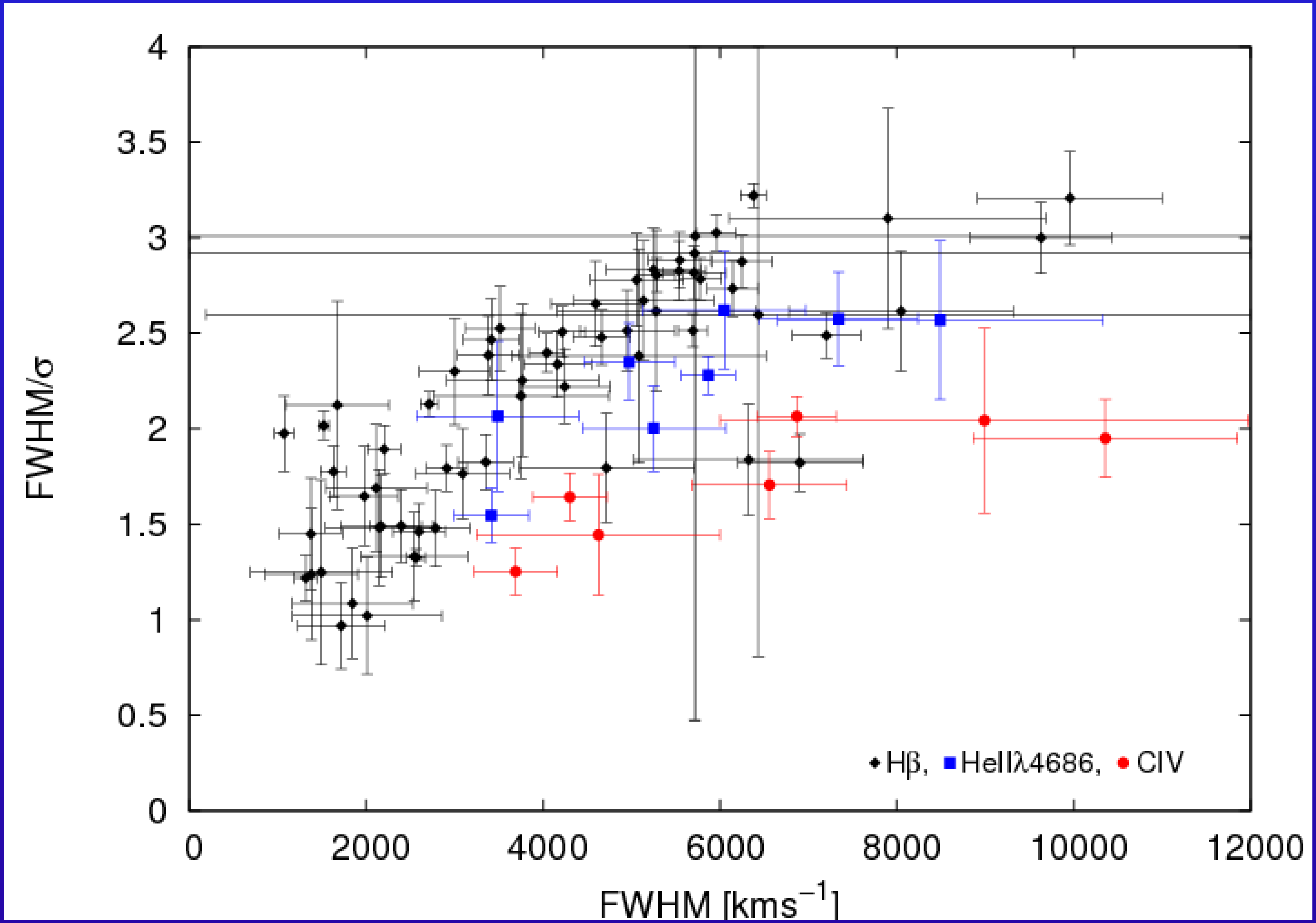

Modeling of observed line profile relations

Tests: *Theoretical line broadening of a Gaussian profile due to rotation and Doppler broadening of a Lorentzian profile .*

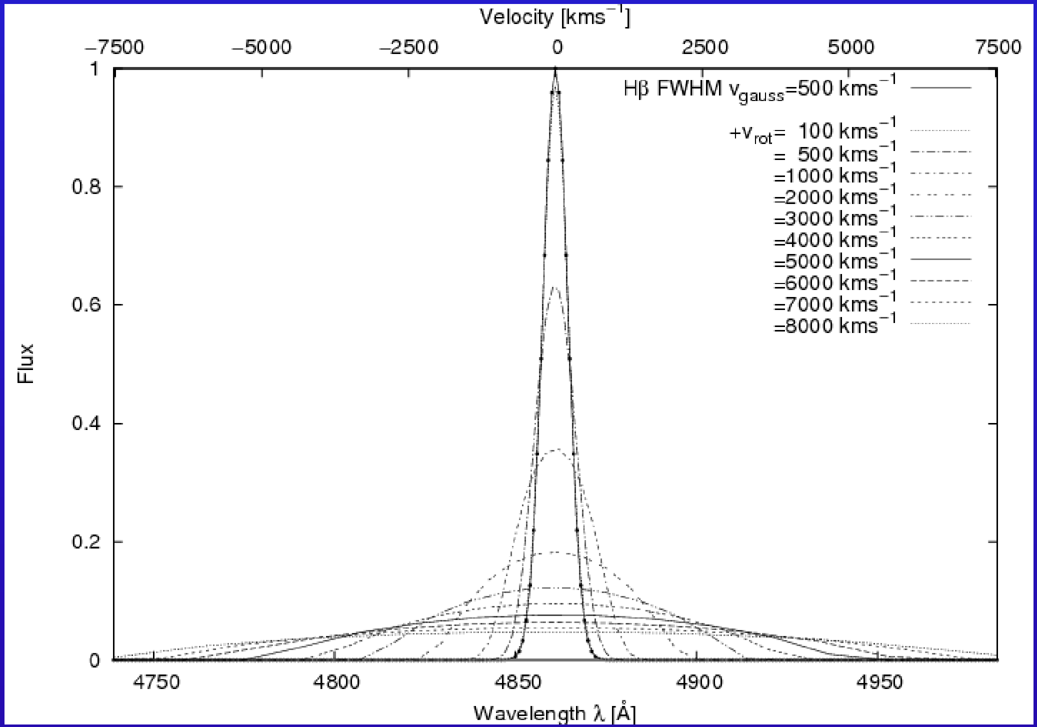

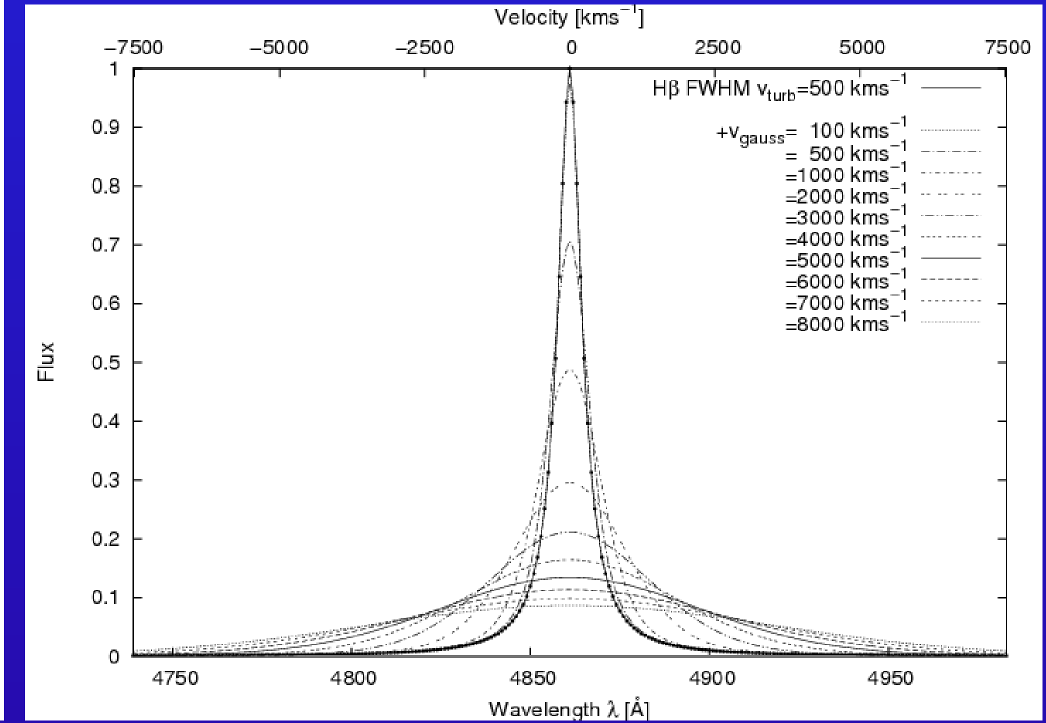

Rotational broadening of a Gaussian Hβ line profile ($v_{Doppler}$ = 500 km/s).

Doppler line broadening of Lorentzian Hβ profile (v_{turb} = 500 km/s).

Modeling of observed line profile relations

Tests: *Theoretical line broadening of Lorentzian profiles due to rotation.*

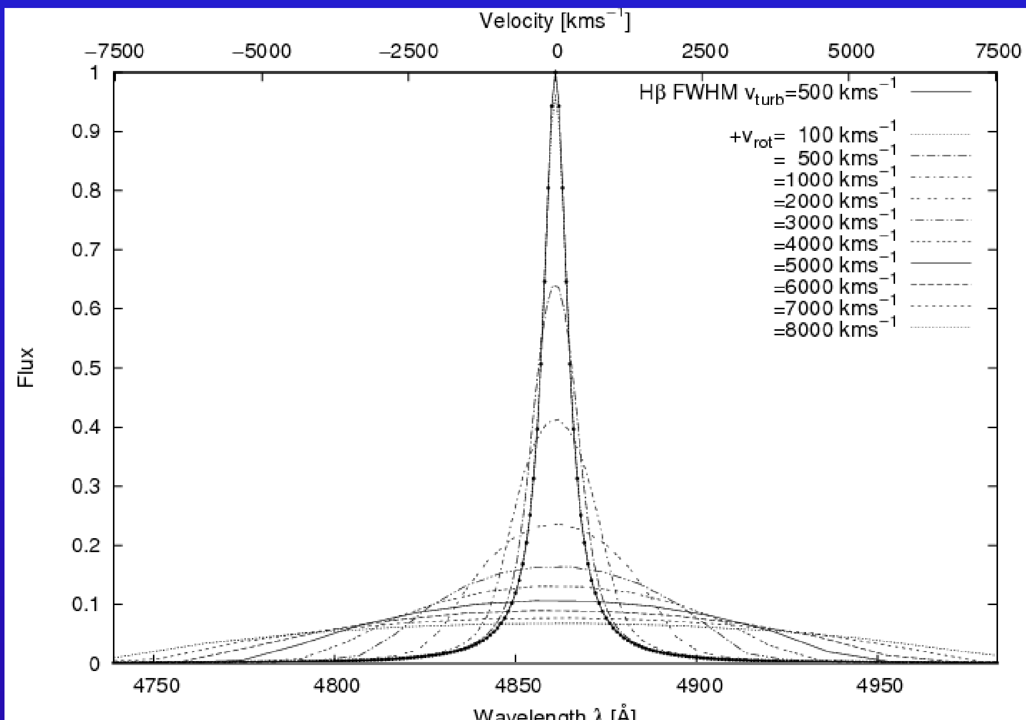

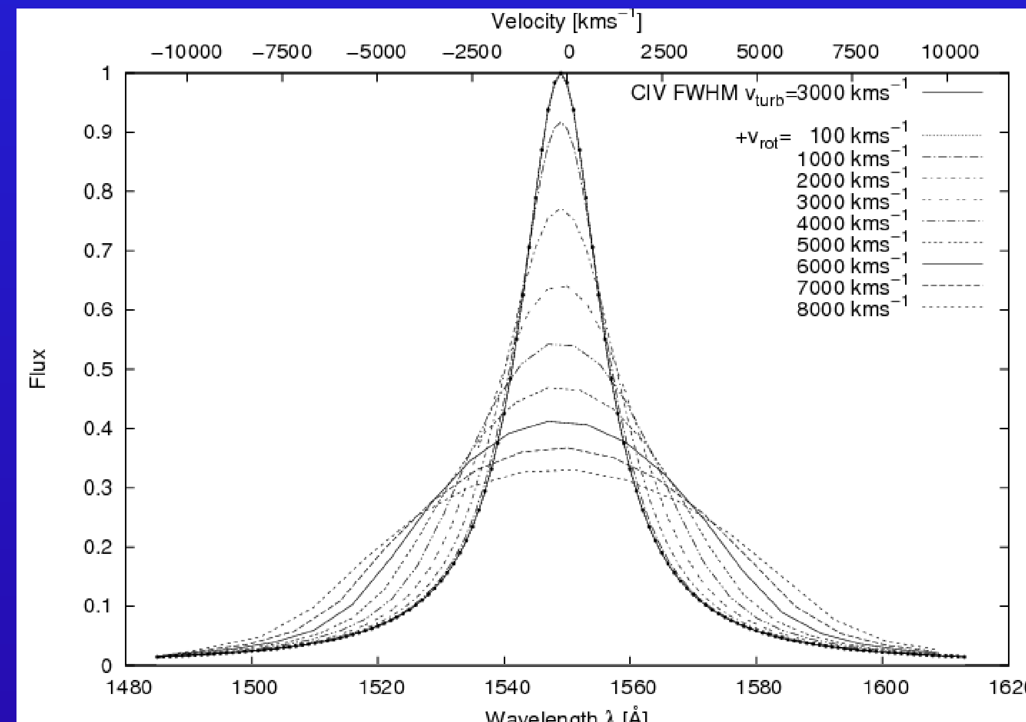

Rotational line broadening of Lorentzian Hβ profile (v_{turb} = 500 km/s).

Rotational line broadening of Lorentzian CIVλ1550 profile (v_{turb} = 3000 km/s).

Modeling of observed line profile relations

in simple way by multiple combinations of profiles.

Observed and theoretical Hβ line-width ratios FWHM/σ versus FWHM

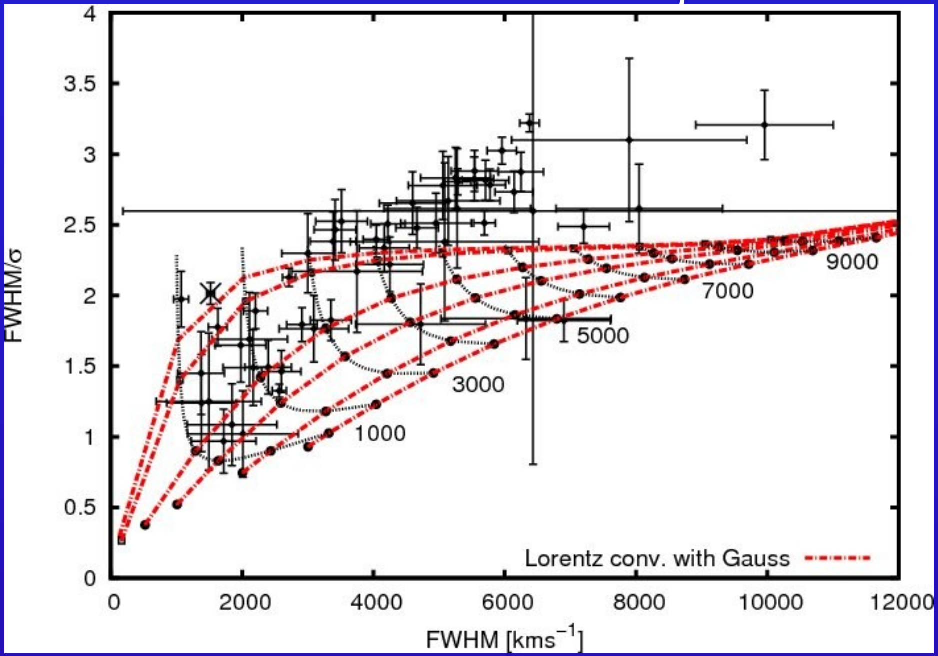

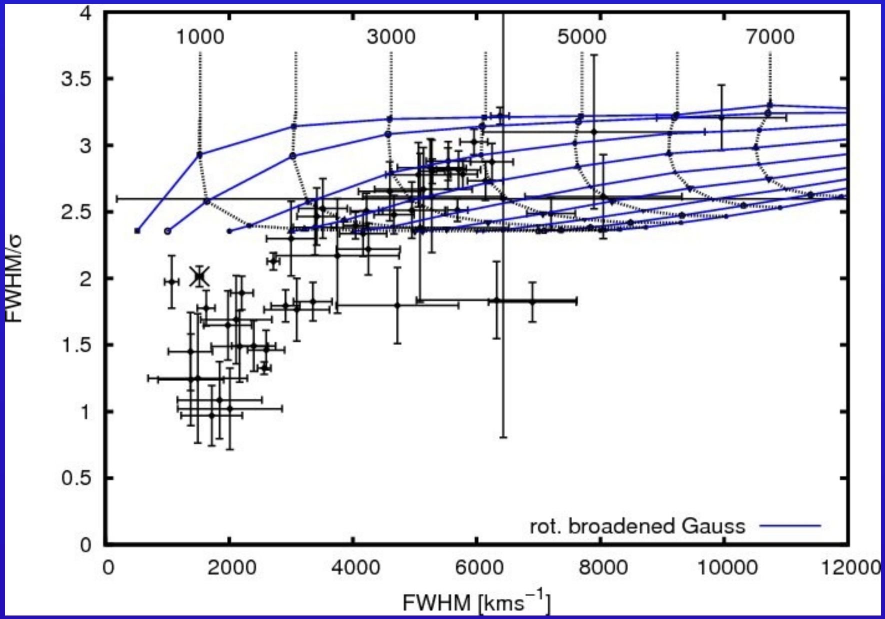

Lorentzian profiles convolved with Gaussian profiles.

The line widths of the Lorentzian profiles (FWHM) correspond to 50, 100, 500, 1000, 2000, 3000 km/s (from top to bottom). The widths of the Gaussian profiles correspond to 1000 to 9000 km/s (from left to right).

Rotational broadening of Gaussian profiles.

The line widths of the Gaussian profiles (FWHM) correspond to 500, 1000,..., 8000 km/s (from top to bottom). The associated rotational velocities range from 1000 to 7000 km/s (from left to right). FWHM/σ always larger than 2.35.

Kollatschny & Zetzl, 2011, Nature 470

Observed and modeled Hβ line widths ratios

General trends: FWHM/σ versus linewidth FWHM

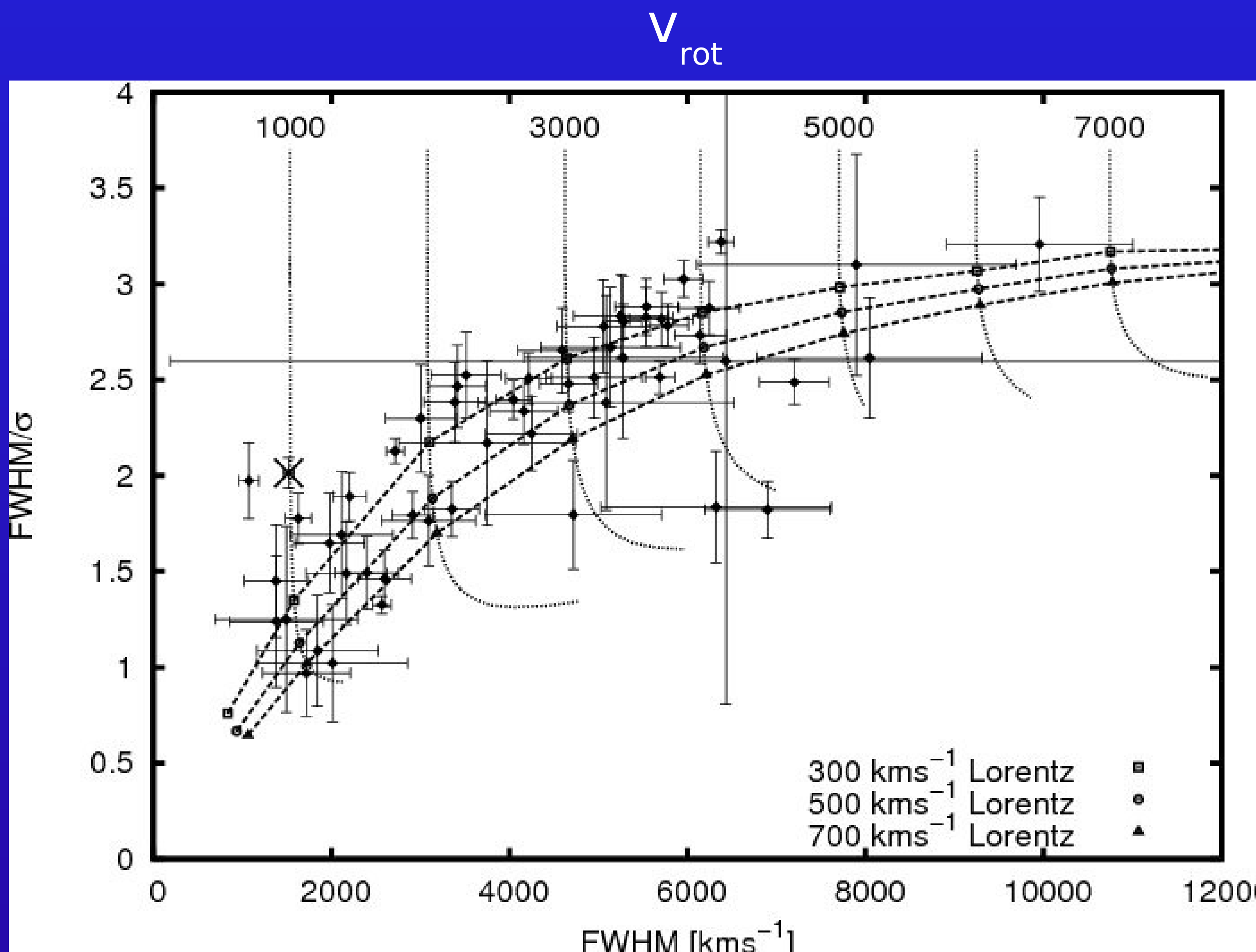

Dashed curves: rotational line broadened Lorentzian profiles (FWHM = 300, 500, 700 km/s). Rotational velocities range from 1,000 to 7,000 km/s.

Kollatschny & Zetzl, 2011, Nature 470

Observed and modeled HeII and CIV line widths ratios

FWHM/σ versus linewidth FWHM

HeIIλ4686

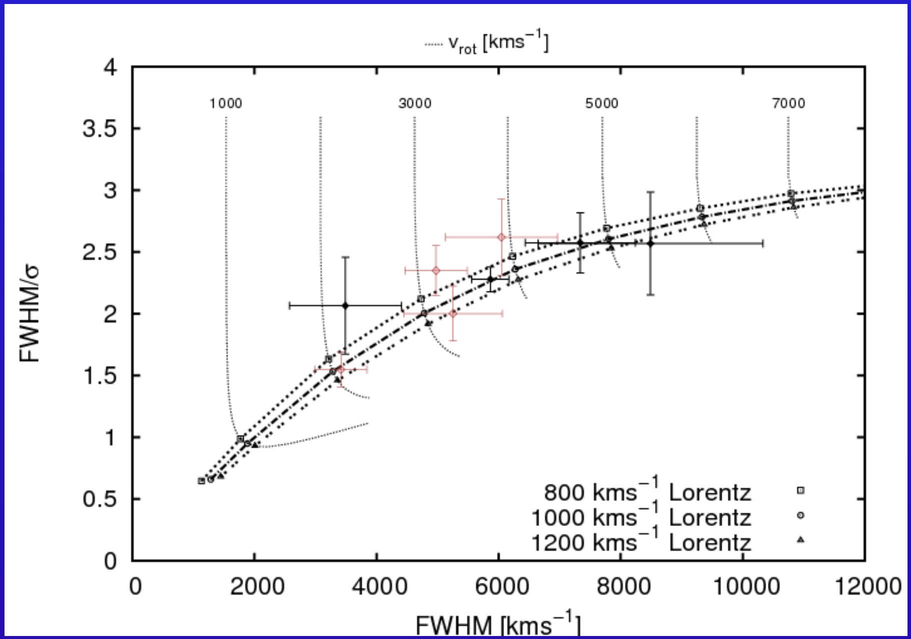

Dashed curves: theoretical linewidth ratios of rotational line broadened Lorentzian profiles (FWHM = 800; 1,000; 1,200 km/s). Rotational velocities range from 2,000 to 6,000 km/s.

CIVλ1550

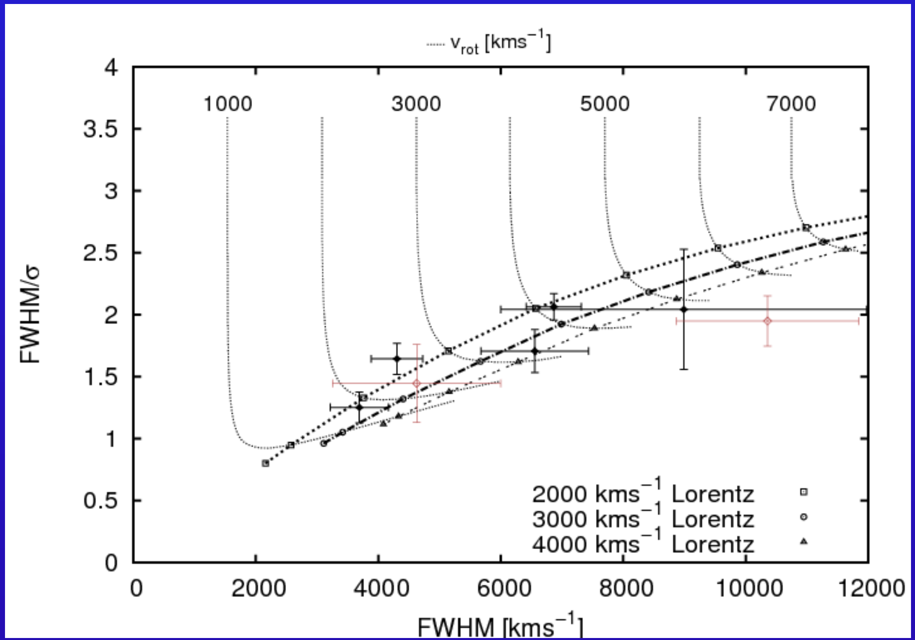

Dashed curves: theoretical linewidth ratios of rotational line broadened Lorentzian profiles (FWHM = 2,000; 3,000; 4,000 km/s). Rotational velocities range from 1,000 to 6,000 km/s.

Line profile studies: BLR structure & kinematics

Observed and modeled Hβ, HeII and CIV line-width ratios FWHM/σ versus linewidth FWHM.

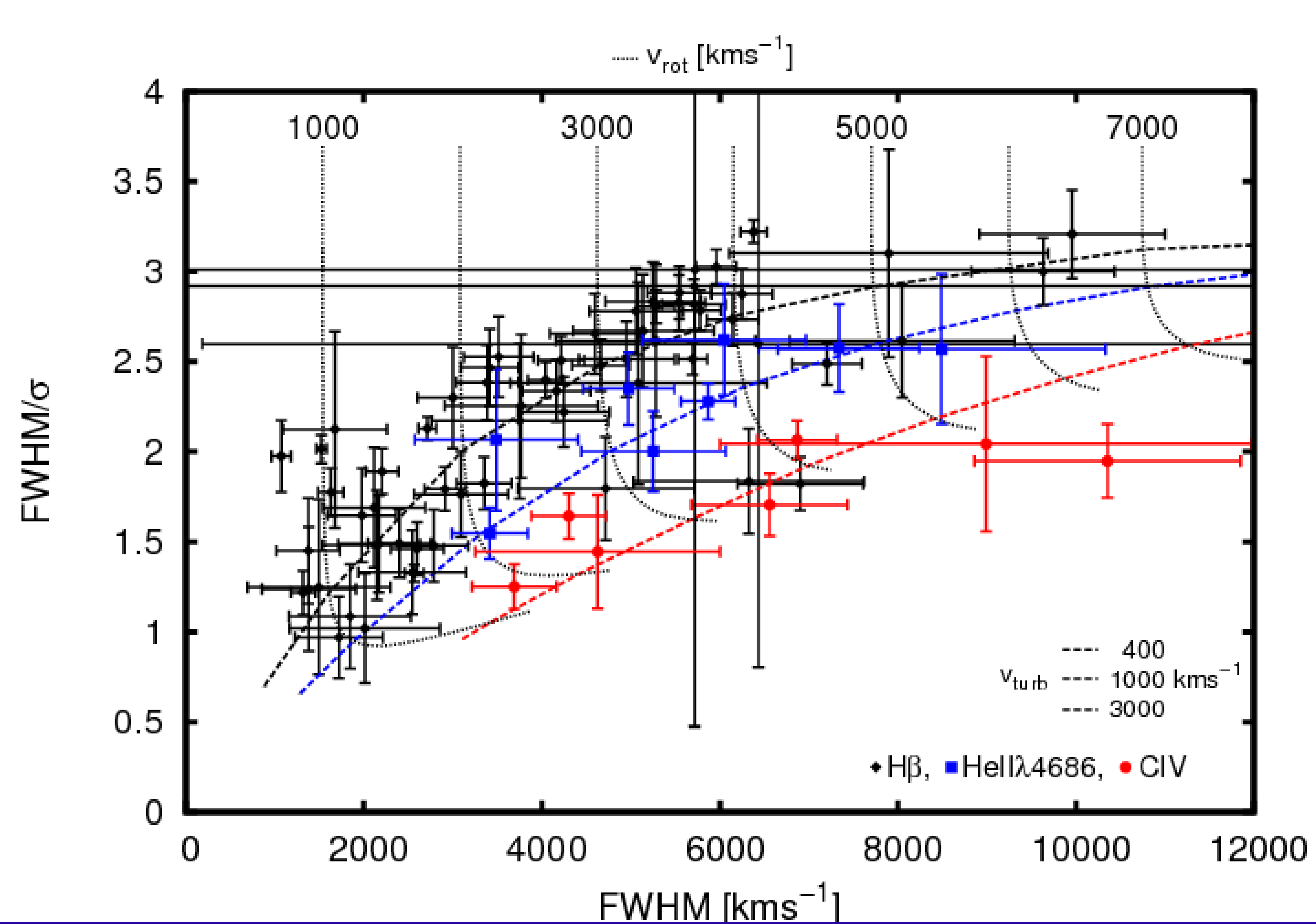

Line profile studies: BLR structure & kinematics

Characteristic turbulent velocities belong to individual emission lines in BLR of all AGN:

- Hβ : 500 ± 200 km/s
- HeIIλ4686 : 1000 ± 200 km/s
- CIII]λ1909 : 1500 ± 700 km/s
- CIVλ1549 : 3000 ± 1000 km/s
- HeIIλ1640 : 3000 ± 1500 km/s
- Lyα+NVλ1240 : 5000 ± 2000 km/s

Emission lines originate at different distances from center in individual galaxies (from reverberation mapping): →

Turbulent velocity varies as function of distance to center.

Kollatschny, Zetzl 2012, subm.

Observed and modeled Hβ line widths ratios

FWHM/σ versus linewidth FWHM

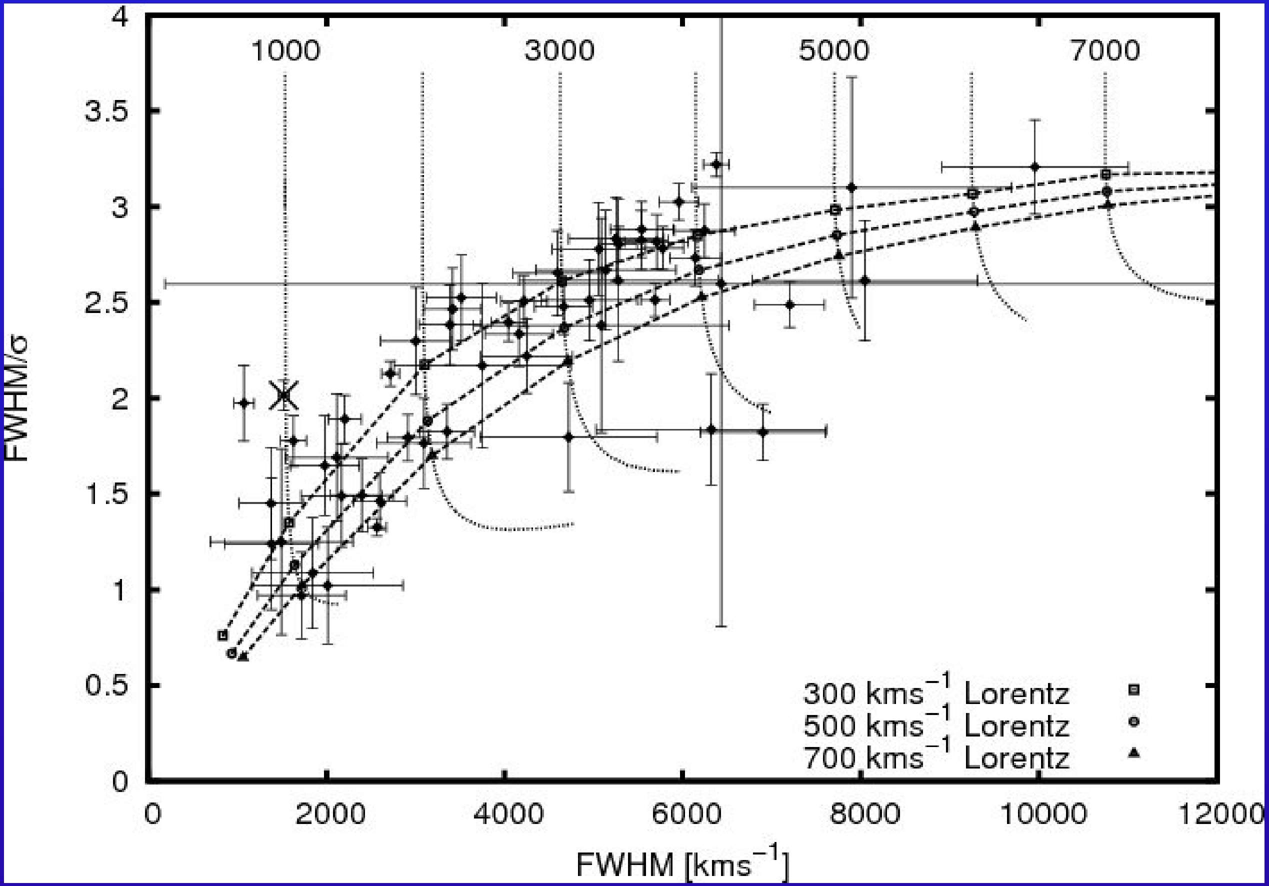

In all AGN: Hβ turbulent velocity ~ 500 km/s

However, rotation velocity different in individual galaxies: 500 – 7000 km/s

Line profile studies: BLR structure & kinematics

Observed and modeled Hβ line-width ratios FWHM/σ versus line-width FWHM.

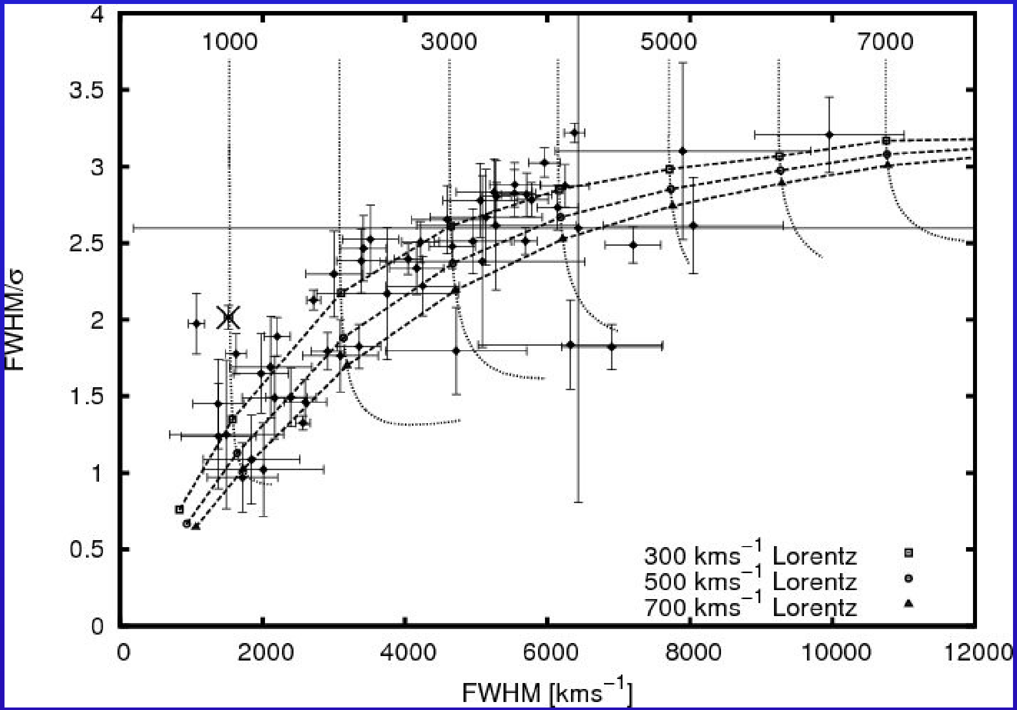

Deviations from general trend by e.g. orientation effects of line-em. accretion disk:
An inclined accretion disk leads to smaller line-widths owing to projection effects while the FWHM/σ remains constant (e.g. Mrk110 marked by a cross (i ~ 21°)).

Further deviations by e.g. additional inflow/outflow components, obscuration,....

Correction factor for black hole masses

v_{rot}

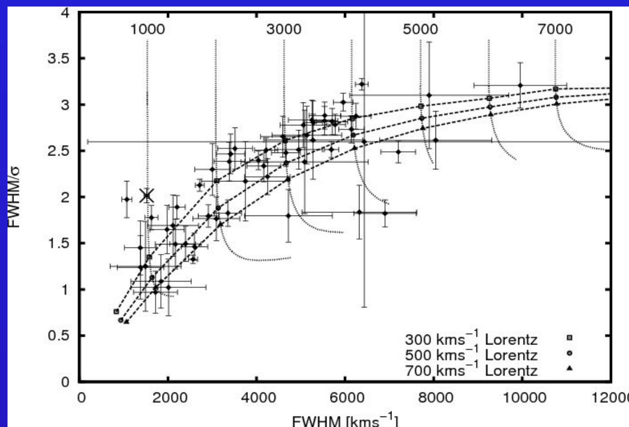

Hβ

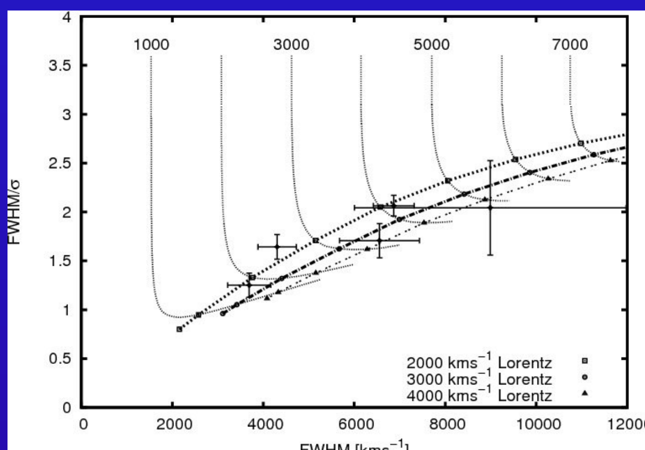

CIVλ1549

$$M = \frac{f V_{\mathrm{FWHM}}^2 c\tau}{G}$$

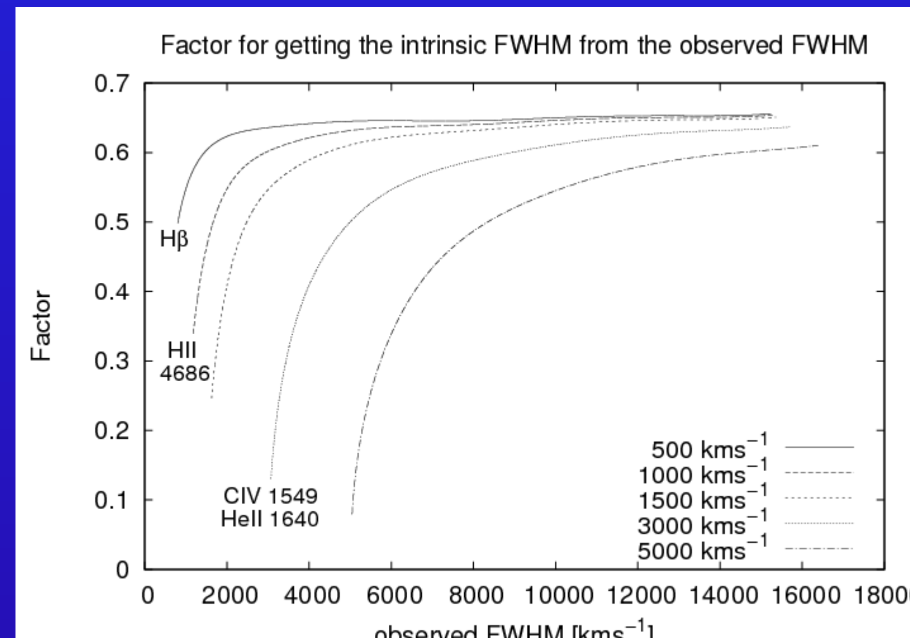

FWHM-correction factor for different em. lines (e.g. Hβ, CIVλ1549) for deriving the BH mass

Kollatschny & Zetzl, 2012, subm.
collab. with Z. Alvi, 2012

- *narrow CIVλ1549 lines are rare (~2%) compared with narrow Hβ (~20%)* *(Baskin & Laor, 2005)*
- *different mass scaling relations are needed for the CIVλ1549 and Hβ line* *(Vestergaard .., 2006)*
- *the use of the CIVλ1549 line gives considerably different BH masses compared to Hβ* *(Netzer et al., 2007)*

Line profile studies: BLR structure & kinematics

From accretion disk theory (e.g. Pringle, 1981):

$$H(eight) / R(adius) = 1/\alpha \ * v_{turb} / v_{rot}$$

α = (const.) viscosity parameter

→ fast rotating broad line AGN: *geometrically thin accretion disk*

→ slow rotating narrow line AGN: *geometrically thick accretion disk*

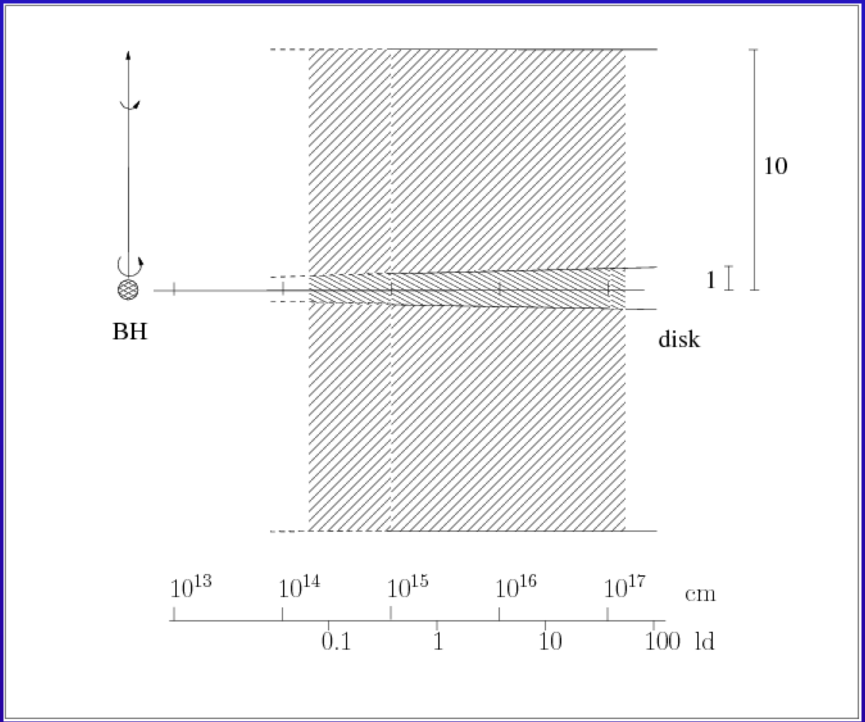

Kollatschny & Zetzl, 2012, subm.

Modeling of individual observed line profiles

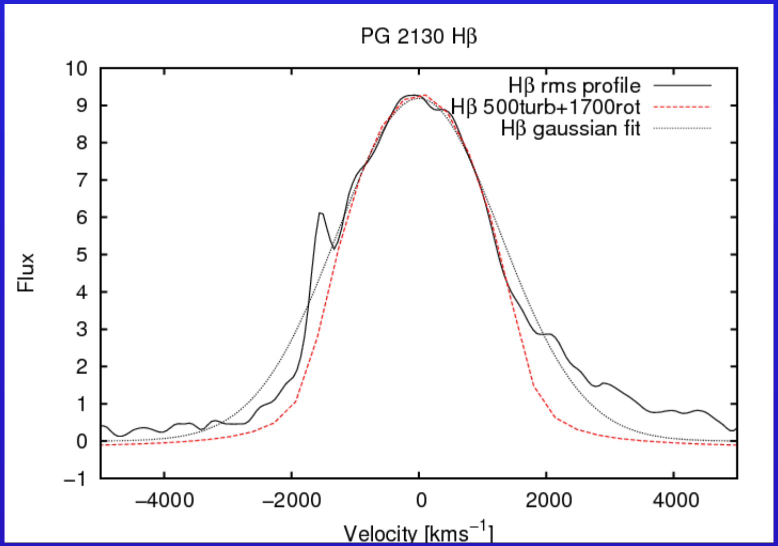

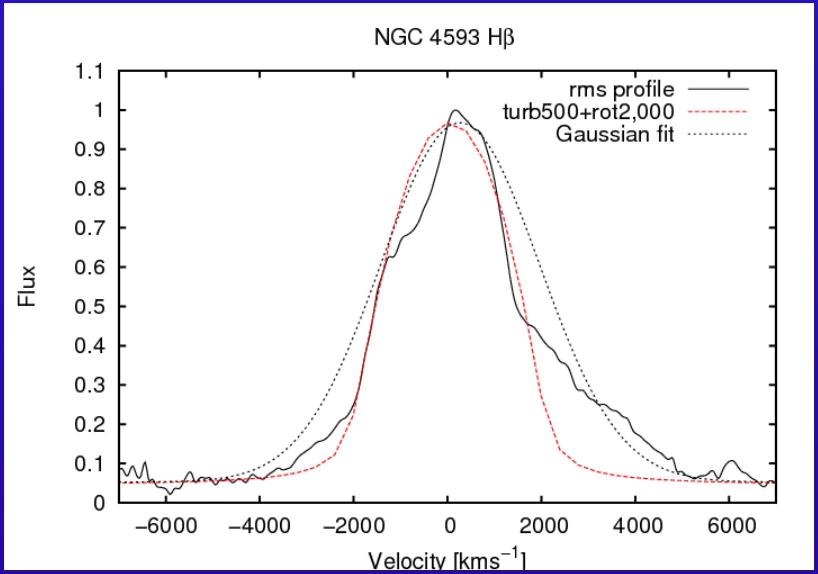

Kollatschny, Zetzl 2011, in prep

GH08

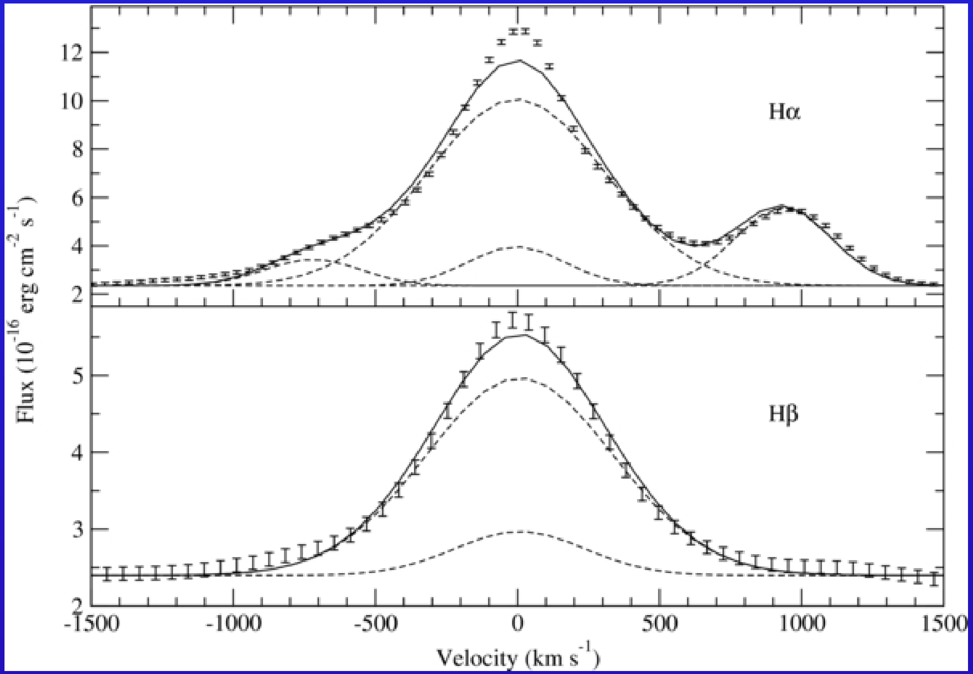

Top: the black data points are the Hα mean velocity profile, the dotted lines are the Gaussian fit for each component, and the solid line is the total fit to the line profile. Bottom: same as above but for the Hβ mean velocity profile. Both fits fall short at the peak due to fitting with pure Gaussians.

Rafter, Kaspi, Behar, Kollatschny, Zetzl 2011

Modeling of narrow line profiles with Lorentzian – not Gaussian - profiles.

Veron et al., 2001, Sulentic et al., 2002, Kollatschny & Zetzl, 2011, Nature

Line profile studies: BLR structure & kinematics

from general line profile trends

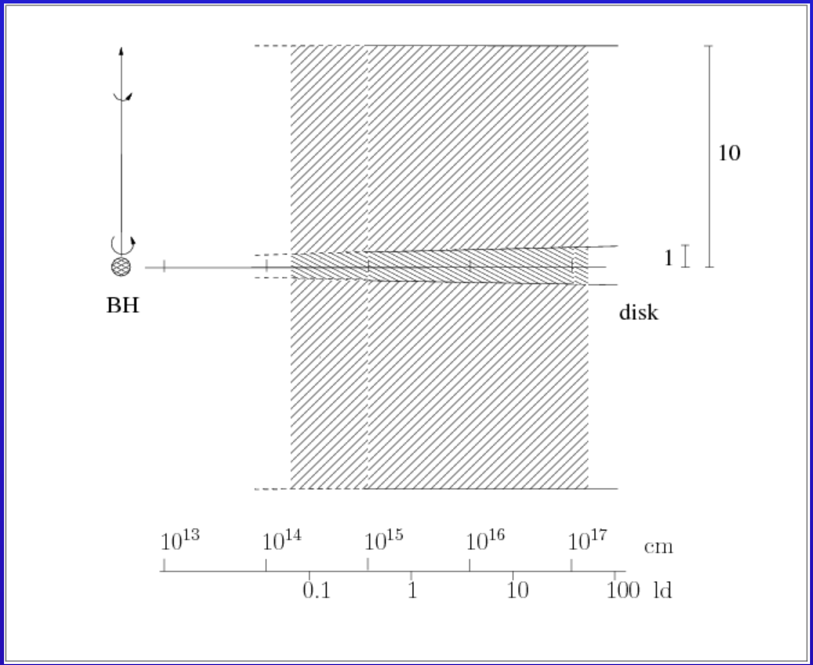

from variability studies

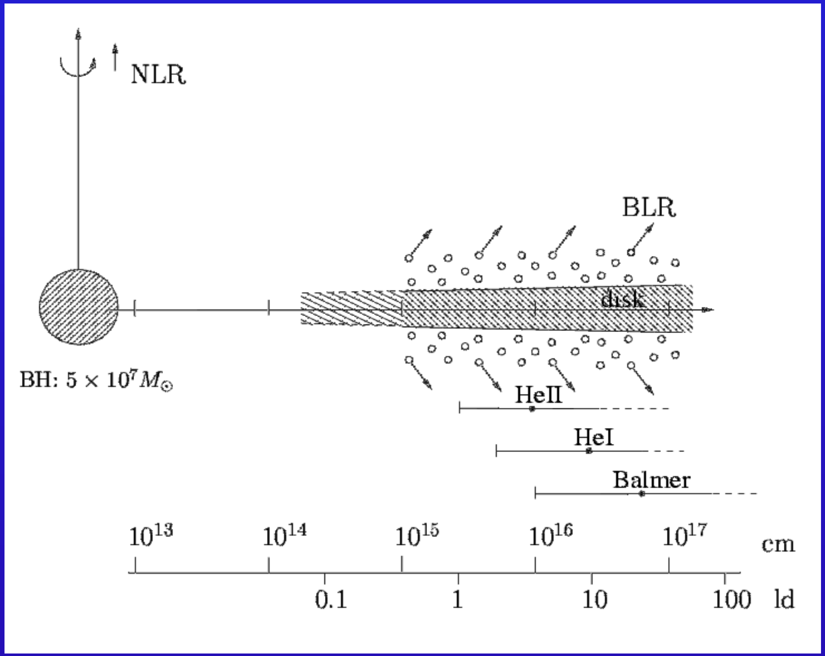

Different Hβ line widths → different rotational vel. → different BLR geometries:

Eigenvector 1 correlation between linewidth, strong FeII emision, soft X-ray excess: due to different BLR/disk geometries !

Kollatschny & Zetzl, 2011, Nature 470, p. 366
2012, subm.

Observed and modeled HeII and CIV line widths ratios

FWHM/σ versus linewidth FWHM

HeIIλ1640

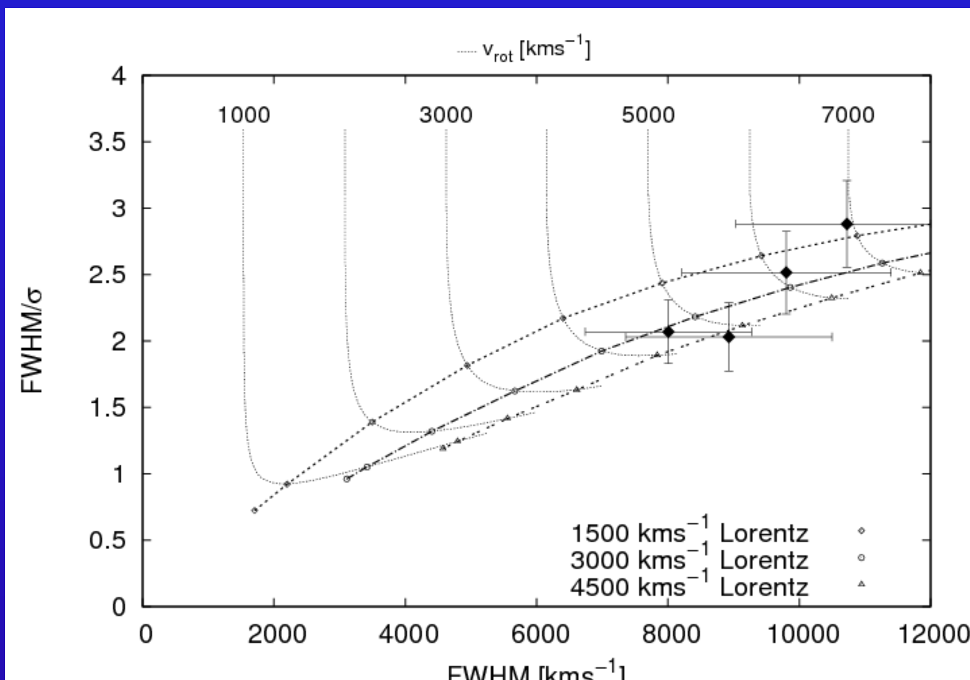

Dashed curves: theoretical linewidth ratios of rotational line broadened Lorentzian profiles (FWHM = 1,500; 3,000; 4,500 km/s). Rotational velocities range from 4,000 to 7,000 km/s.

Lyα

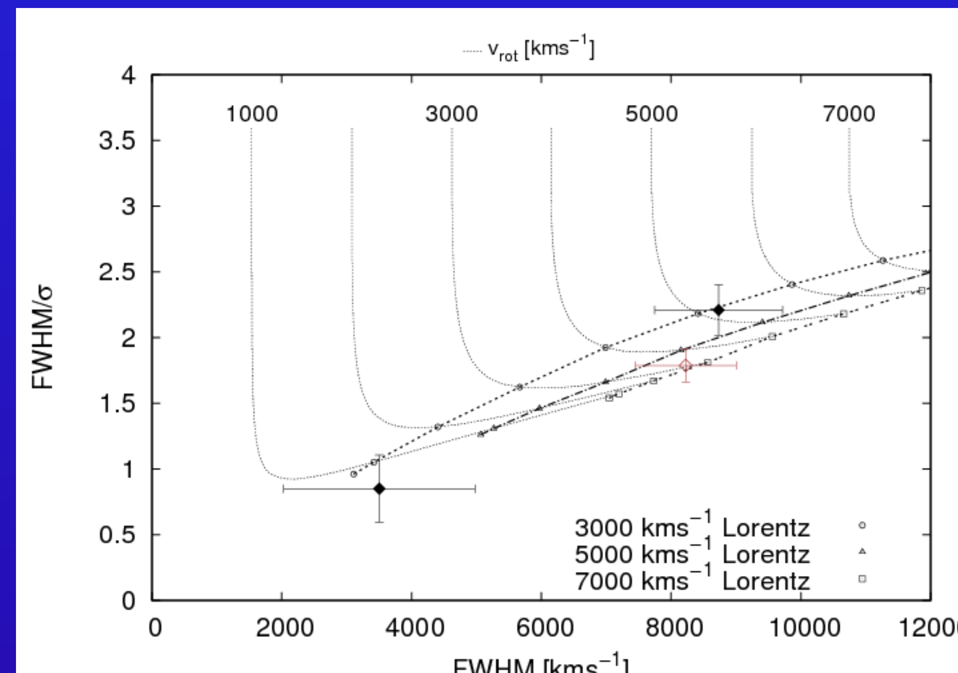

Dashed curves: theoretical linewidth ratios of rotational line broadened Lorentzian profiles (FWHM = 2,000; 3,000; 4,000 km/s). Rotational velocities range from 1,000 to 6,000 km/s.